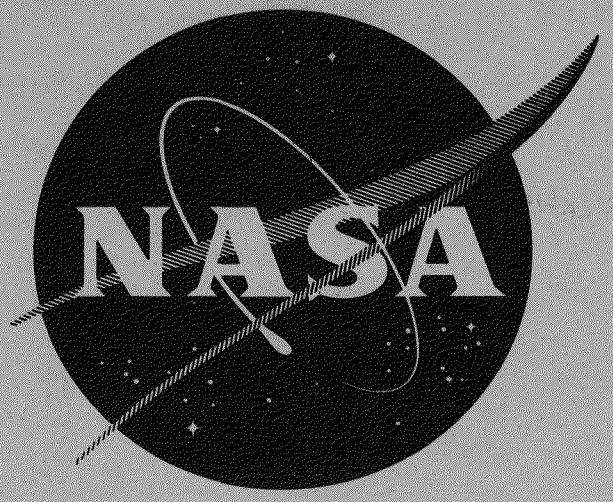

GA-4874

STUDIES OF THERMIONIC MATERIALS FOR SPACE POWER APPLICATIONS

Quarterly Progress Report for the Period
September 1, 1963, through November 30, 1963

by

Members of the Direct Conversion Project

Prepared for
National Aeronautics and Space Administration
Lewis Research Center
under Contract NAS3-4165

GENERAL ATOMIC
DIVISION OF
GENERAL DYNAMICS

JOHN JAY HOPKINS LABORATORY FOR PURE AND APPLIED SCIENCE

P.O. BOX 608, SAN DIEGO 12, CALIFORNIA

DISCLAIMER

GA-4874

STUDIES OF THERMIONIC MATERIALS FOR SPACE POWER APPLICATIONS

Quarterly Progress Report for the Period
September 1, 1963, through November 30, 1963

by

Members of the Direct Conversion Project

Sponsored by
National Aeronautics and Space Administration
Lewis Research Center

Technical Management
NASA – Lewis Research Center
Nuclear Power Technology Branch
J. W. R. Creagh

GENERAL ATOMIC
DIVISION OF
GENERAL DYNAMICS

JOHN JAY HOPKINS LABORATORY FOR PURE AND APPLIED SCIENCE

P.O. BOX 608, SAN DIEGO 12, CALIFORNIA

Contract: NAS3-4165
Issued: February 28, 1964

NOTICES

This report was prepared as an account of Government-sponsored work. Neither the United States nor the National Aeronautics and Space Administration (NASA), nor any person acting on behalf of NASA:

A) Makes any warranty or representation, expressed or implied, with respect to the accuracy, completeness, or usefulness of the information contained in this report, or that the use of any information, apparatus, method, or process disclosed in this report may not infringe privately-owned rights; or

B) Assumes any liabilities with respect to the use of, or for damages resulting from the use of any information, apparatus, method or process disclosed in this report.

As used above, "person acting on behalf of NASA" includes any employee or contractor of NASA, or employee of such contractor, to the extent that such employee or contractor of NASA or employee of such contractor prepares, disseminates, or provides access to, any information pursuant to his employment or contract with NASA, or his employment with such contractor.

AVAILABILITY NOTICE

Qualified requestors may obtain copies of this report from:

National Aeronautics and Space Administration
Office of Scientific and Technical Information
Washington 25, D. C.
Attn: AFSS-A

TABLE OF CONTENTS

LIST OF FIGURES

List of Figures--continued

List of Figures--continued

LIST OF TABLES

FOREWORD

Contributors to this report are as follows:

L. Yang, Principal Investigator

R. W. Pidd, Direct Conversion Project Manager

Section I:
- A. F. Weinberg, Coordinator
- J. R. Lindgren

Section II:
- L. Yang, Coordinator
- F. D. Carpenter
- P. E. Gethard
- R. G. Hudson
- R. C. Weed
- L. R. Zumwalt

Section III:
- J. W. Holland, Coordinator
- M. H. Horner
- J. T. Ream
- R. Skoff
- A. F. Weinberg

Section IV:
- W. W. Godsin, Coordinator
- J. T. Ream
- W. B. Wright
- L. Yang

SUMMARY

The work accomplished during the first quarter of Contract NAS 3-4165 (September 1, 1963, to November 30, 1963) is summarized as follows.

1. Fabrication Development

Isostatic-pressing techniques using reversible gels as the pressing medium have been studied for improving the uniformity in density and structure of UC-ZrC bodies. Control of powder-size fraction was studied as a means for controlling the pore distribution. Low-pressure krypton adsorption was used to characterize the total surface areas of the samples prepared. Control of carbon content of UC-ZrC samples by thermal treatment in a mixture of H_2 and hydrocarbon has been studied. Preparation of near stoichiometric 30 UC – 70 ZrC powder by gas–metal reaction has been demonstrated.

Assembly of an apparatus for the study of the thermochemical vapor-deposition of tungsten is near completion. A research and development subcontract on the same subject is being negotiated with San Fernando Laboratories.

2. Studies of High-Temperature Properties of Thermionic Materials

The vaporization and fission-product (Xe^{133}, Te^{132}, I^{131}, Ba^{140}) release rates of a hot-pressed high-density (~97% theoretical density) 30 UC – 70 ZrC sample, A_1, have been measured in the temperature range 1800° to 2000°C.

A low-pressure gas adsorption apparatus has been set up for measuring the true surface area of UC-ZrC samples.

The cell used for the study of fission-product diffusion through tungsten clad has been fabricated, and the counting equipment has been ordered.

Preparation of the samples needed for fuel–clad compatibility and refractory-metal interdiffusion studies has been partially completed. A high-temperature furnace has been ordered for long-term compatibility studies.

Diffusion-emission studies have been made on a rhenium-clad UC (4.63% carbon) sample (E_1) at 1800°C. The diffusion-emission cell for studying the rhenium- and iridium-coated tungsten samples has been fabricated.

The molybdenum pedestal of the loading device of the high-temperature mechanical testing furnace has been modified. The new pedestal is being fabricated.

Thermionic emission microscopy shows that areas of high work-function can co-exist with better-emitting UO_2 dispersions on the surface of a W-UO_2 cermet at 1650°C.

3. Life-Testing of Fueled Cesium Converters

Life-testing cells using planar, as well as cylindrical, fueled emitters have been designed. Fabrication development has been carried out on both types of emitters.

The cylindrical configuration is favored, since a reliable cylindrical-cell envelope has been developed. Testing stations have been designed, and ordering of the equipment is under way.

4. Irradiation Studies

A manuscript has been assembled and submitted to the Policy Committee of the Plum Brook Reactor Facility for its approval on using the Plum Brook Reactor for the irradiation experiments under this contract.

INTRODUCTION

This report covers the work accomplished during the first quarter of Contract NAS 3-4165. This contract is a continuation of the work carried out under Contracts NAS 3-2532,[1] NAS 5-1253,[2] and NAS 3-2301.[3] The goal of the work under all the contracts is to develop thermionic cathode materials of useful life and performance for the direct conversion of fission heat to electrical energy for space power applications. Lists of the previous reports issued under these contracts can be found at the front of the final reports on each of these contracts.[1][2][3]

Emphasis under the present contract is placed on four major areas. These are

1. Fabrication development of the UC-ZrC fuels and vapor-deposited tungsten clad so that thermionic cathodes of desired properties can be obtained reproducibly.
2. Studies of the high-temperature properties of thermionic materials. This includes (a) the effect of structures of fuels and clad materials on their vaporization, fission-product release, and fission-product diffusion properties, (b) general mapping of the temperature range of materials compatibility between various fuels and refractory metals and alloys, (c) mechanical properties of UC-ZrC at high temperatures, (d) emission microscopy studies of tungsten–(uranium-containing carbide) cermet surfaces.
3. Life-testing of fueled cesium thermionic cells for their performance stability at a power output of better than 5 watts/cm^2, with a goal of 10,000-hr operation.
4. Irradiation studies of candidate thermionic cathode materials to fission densities equivalent to 5000-hr thermionic fuel element life.

Section I

FABRICATION DEVELOPMENT

The investigations described in this section relate to continuing efforts to improve the fabrication of fuels and metal claddings by achieving greater understanding of the influence of fabrication variables on the properties of the end product and utilization of this understanding to control and improve these properties. Studies currently in progress are restricted to those materials used in the emitter structure, and include refractory carbide fuels as well as the technology of vapor-deposited tungsten.

1.1. FUEL DEVELOPMENT

In the last three years, carbide fabrication has developed through several stages:

(1) Lack of almost all control, all efforts being devoted to making carbide specimens of any kind--no matter what the properties.

(2) The beginnings of composition control, i.e., relating the final composition to the composition of the starting material and sintering cycle.

(3) Control of density by controling the sintering cycle.

At all stages, primary concern was to make the best-quality product possible with respect to purity, structure, and composition, and, in all cases, even where it was not possible to completely control all properties, at least to characterize them as fully as possible. Little effort was expended in relating the techniques employed to the economics of large-scale production.

At the end of the last contract period (August 31, 1963), three problem areas still remained which were deemed to be of major importance:

1. Pressing. The technique employed was the use of a split-die arrangement, with double-acting plungers. This arrangement had a number of disadvantages:

a. Non-uniformity of density and structure in a radial direction, because the vertical motion of the plungers did not cause any pressure in the radial direction.

b. Non-uniformity in a vertical direction, since the relative motion of the powders is greatest at the ends of the compact and smallest in the central region.

c. Limitation of the length-to-diameter ratios which could be pressed; as the length-to-diameter ratio increases, the non-uniformity in vertical direction becomes prohibitively excessive.

d. Structural faults resulting at the junctions of the die segments.

e. Little flexibility of dies, and high die costs; each time that a new dimension was required, a new, expensive die was required.

f. Limitation to simple shapes; only extremely simple shapes can be made, which requires much machining and material waste when it is necessary to fabricate more complex shapes such as cups or tubes.

2. Pore Distribution Control. The need for structures having open porosity to facilitate fission-gas release and prevent swelling has been demonstrated. The only control over the pore structure, however, was through control of the density obtained during sintering; and more control is required. In addition, better means of characterizing the pore distribution in specimens was required than the mercury porosimetry techniques used to date.

3. Composition Control for Hyperstoichiometric Carbides. Control of carbon content in hypostoichiometric and stoichiometric carbides could be obtained by allowing the carbide powder to oxidize, causing the formation of CO during sintering and the reduction of the carbon content to the point where liquid uranium is formed. This is followed by coordinating the final heat-treatment temperature with the phase diagram so that the excess uranium is boiled off until one enters the single-phase region at the carbon composition desired. This was only useful for hypostoichiometric or stoichiometric carbides, and little control was being maintained in those cases where hyperstoichiometric carbon contents were required.

Research programs were formulated to solve these problems and each is described below.

1.1.1. Powder Pressing

Isostatic pressing, an old ceramic and powder metallurgy technique, was known to be capable of solving all of the pressing problems enumerated above if it could be put to use. The pressures employed in commercial isostatic pressing equipment (using fluids in a pressurized system), however, were of the order of 20,000 psi, whereas carbides have required pressures on the order of 60,000 to 100,000 psi. To obtain equipment

producing pressures of that magnitude was prohibitively expensive; therefore, other techniques were desired.

T. W. Penrice[4] reports on the use of reversible gels to provide an isostatic pressing medium which could be used in simple dies on a conventional press. This is shown schematically in Fig. 1.1. Although only unidirectional pressure is applied, the gel, being incompressible, acts as an isostatic medium and applies pressure to the powder equally in all directions. This technique appeared to be quite adaptable to our needs, and studies were begun. During this reporting period, most of the work was devoted to learning the techniques and vagaries of the method.

The first problem encountered was to obtain a gel having the characteristics requisite to this application. General Electric RTV silicone rubber was tried, but its strength was not sufficient to take the loads required. Plaschem "Chemsol," a polyvinyl chloride, is currently being used and appears quite satisfactory; however, Mobay Multrathone, a urethane, has been ordered for evaluation. All of these materials set at room temperature or at moderately elevated temperatures, so that almost any material can be used as the form for the powder cavity. In the case of cylindrical shapes, glass tubing is used both to form the powder cavity and to contain the reversible gel on the outer diameter so that it will fit into the steel die. Only one steel die is required for making a variety of sizes and shapes.

Studies made using ZrC powder indicated that tapered ends were required on the cavity of the isostatic-medium mold in order to consistently produce pressings which did not contain transverse cracks. Careful measurements of pressings made in molds with straight cylindrical cavities showed that the ends were a few thousandths of an inch larger in diameter than the center of the specimen. It is thought that during the initial application of pressure the ends are pressed down first before the mold contacts the steel die wall and begins to exert pressure in an isostatic fashion. This causes a slight bulging of the ends. When the pressure is released after compaction and the mold springs back to its original length and shape, it "hangs up" on the bulged end and pulls the compact apart. Use of the tapered section has eliminated this problem. In addition, tapered sections can be readily removed from the tapered mold through a longitudinal slit on one side of the mold. An isostatically pressed ZrC compact is shown in Fig. 1.2. Specimens made in this manner can be easily centerless-ground to any uniform diameter.

Preliminary evaluation of this technique shows that UC-ZrC compacts of more uniform and higher density can be made by this technique than by ordinary unidirectional pressure application. Figures 1.3(a), (b), (c), and (d) illustrate the uniformity of pore distribution achieved. These photomicrographs are from different parts of sample 20T-3 (see Table 1.3). Table 1.1 lists some of the data obtained to date.

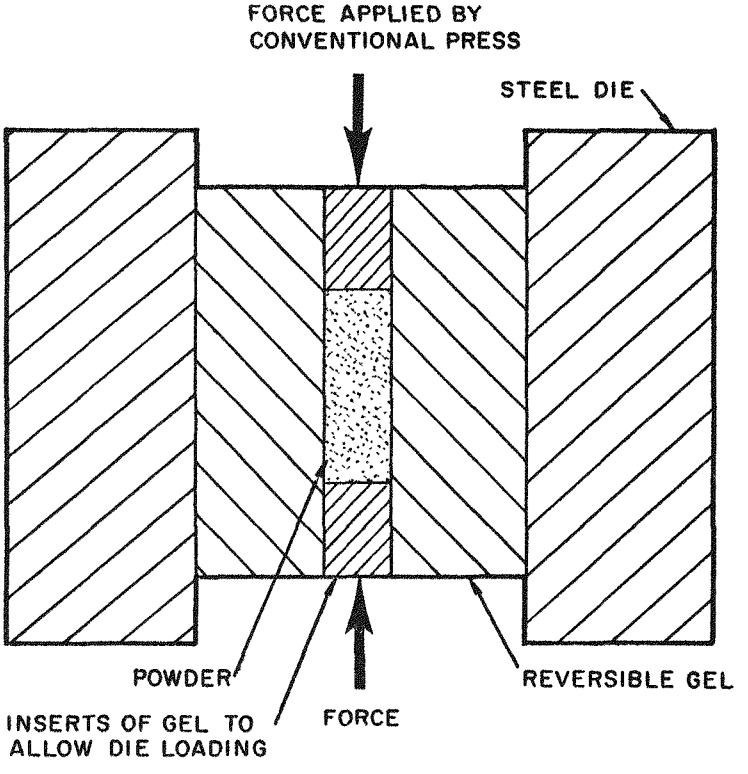

Fig. 1.1--Schematic representation of isostatic pressing utilizing reversible gel as the isostatic medium

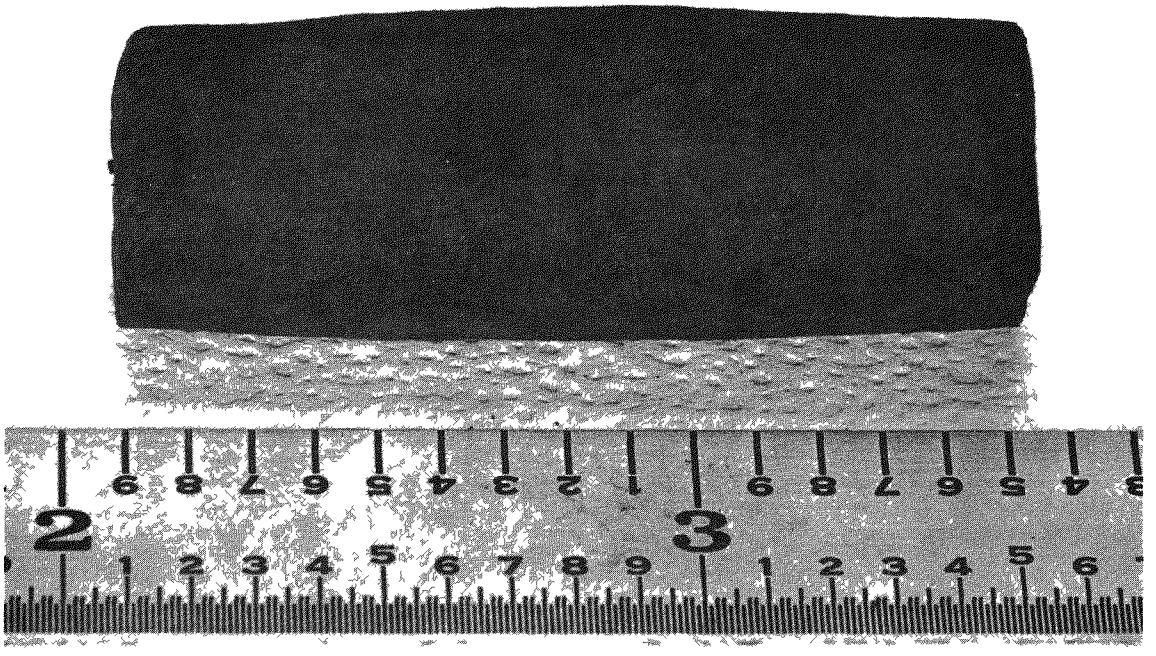

TE-24503

Fig. 1.2--Isostatically pressed ZrC body

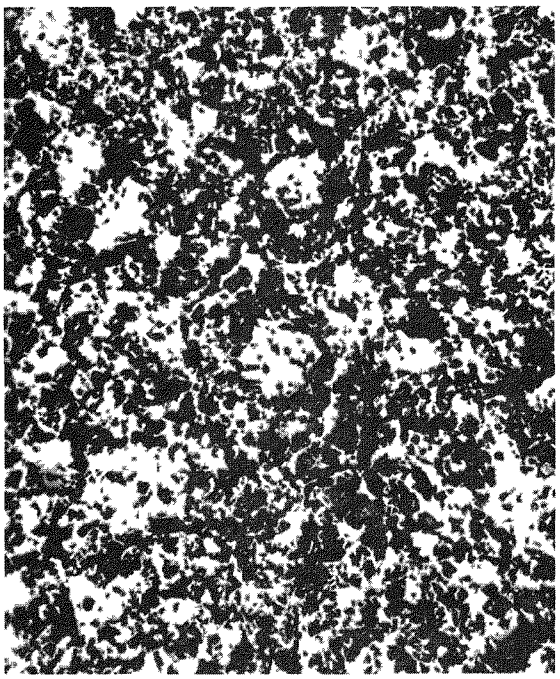

M-5301-1-1 (400×)

(a)

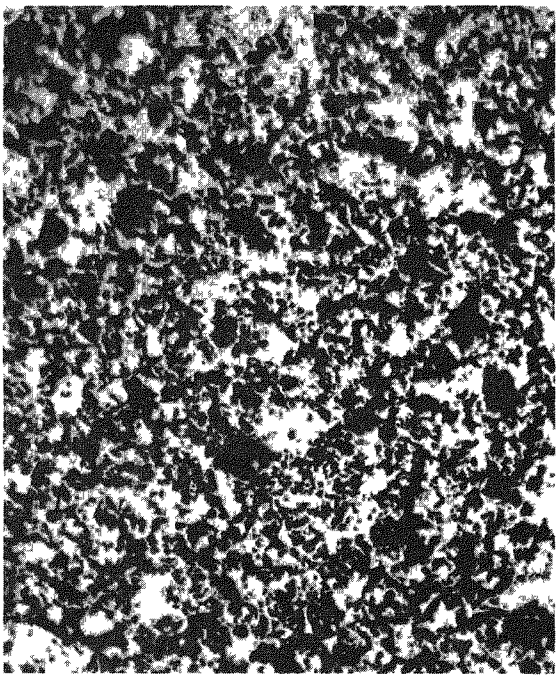

M-5301-1-2 (400×)

(b)

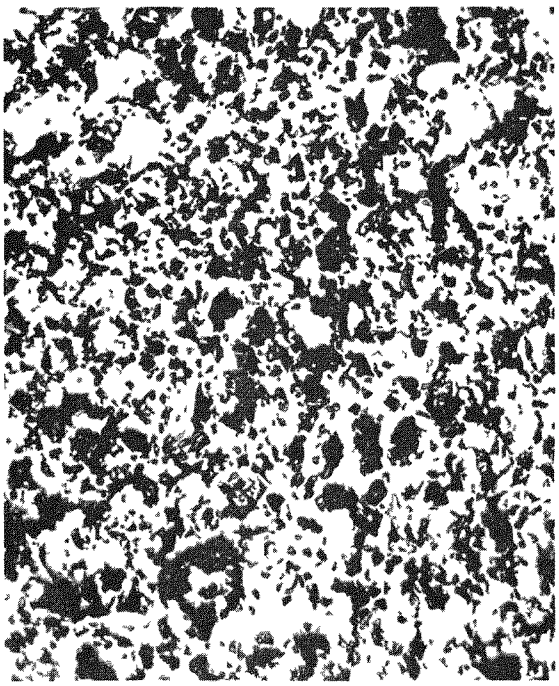

M-5301-2-1 (400×)

(c)

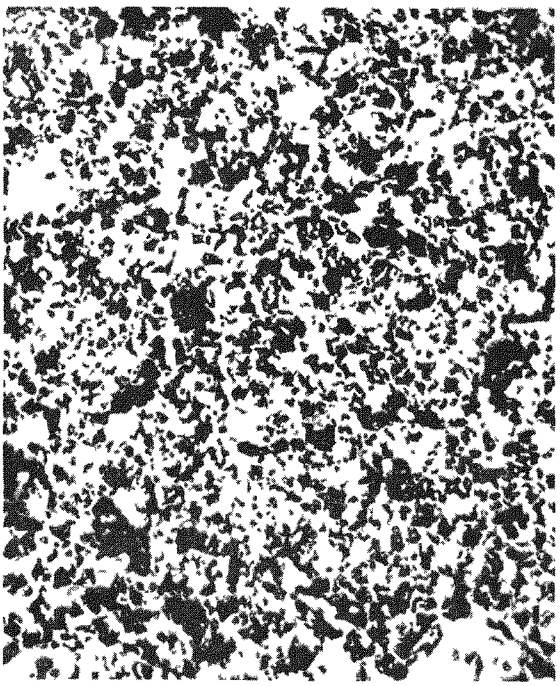

M-5301-2-2 (400×)

(d)

Fig. 1.3--Uniform pore structure obtained in isostatically pressed compacts of 30 UC — 70 ZrC composition

Table 1.1

UNIFORMITY OF SINTERED DENSITIES OF ISOSTATICALLY PRESSED UC-ZrC BODIES

Specimen No.	Composition	Sintered Density (% T.D.)	Ratio of Length to Diameter	Sintering Temp. (°C)
Uniformity of resulting densities in different pressings made under identical conditions				
1074A	30 UC – 70 ZrC	90.0	2:1	2200
1074B	30 UC – 70 ZrC	88.5	2:1	2200
1074C	30 UC – 70 ZrC	89.9	2:1	2200
1074D	30 UC – 70 ZrC	88.5	2:1	2200
Uniform density obtained in sections taken from different longitudinal positions in single pressings of 90-10, 70-30, and 30-70 compositions				
1071-1	90 UC – 10 ZrC	89.5	3.75:1	1900
1071-2	90 UC – 10 ZrC	91	3.75:1	1900
1071-3	90 UC – 10 ZrC	89.5	3.75:1	1900
1066-1	70 UC – 30 ZrC	95.8	3:1	2250
1066-2	70 UC – 30 ZrC	96.7	3:1	2250
1070-1	30 UC – 70 ZrC	91.5	3.75:1	2250
1070-2	30 UC – 70 ZrC	91	3.75:1	2250
1070-3	30 UC – 70 ZrC	91	3.75:1	2250

Systematic studies of the pressing parameters are still required. In addition, preliminary attempts are planned to produce cups, tubes, and other difficult shapes by this technique.

1.1.2. Control of Pore Distribution

Specimen Preparation

The method singled out to be the most direct means of obtaining control over the porosity was control of the powder fraction used. To date, all powders were -325 mesh, i.e., of less than 45μ size and including all smaller powder sizes. Table 1.2 lists the specimens prepared to date. In general, the powder fractions studied have resulted in stable, low-density

bodies. For a given combination of composition and sintering temperature, these densities are lower than would be expected using -45μ powder.

Table 1.2

SINTERED DENSITIES OBTAINED USING DIFFERENT POWDER FRACTIONS

Composition (mol-%)	Powder Fraction (microns)	Sintering Temp. (°C)	Pressing Method*	Density (% theoretical)
90 UC – 10 ZrC	-150/+100	1800	UNI	74.6
	-100/+65	1800	UNI	75.6
	-65/+45	1800	UNI	73.3
	-65/+20	2250	ISO	81-82
	-65/+20	1900	ISO	~80
30 UC – 70 ZrC	-150/+100	1930	UNI	75.0
	-100/+65	1930	UNI	76.6
	-65/+45	1930	UNI	77.2
	-45	~1900	ISO	~81
70 UC – 30 ZrC	-65/+20	2250	ISO	81-82
	-65/+20	1900	ISO	79

*UNI means cold pressed by standard method using unidirectional pressure.

ISO means isostatically pressed in Chemsol mold.

Efforts are being made to produce higher-density bodies while still retaining the open-pore structures required. The two powder fractions to be studied next are -45μ with -10μ and with -20μ powders removed. Both 90 mol-% UC – 10 mol-% ZrC and 30 mol-% UC – 70 mol-% ZrC compositions will be investigated.

Several specimens for this part of the program have been made by isostatic pressing, and very uniform, open-pore structures were observed. The open-pore structure in a 70 UC – 30 ZrC specimen when -65μ/+20μ powder fraction was used is shown in Fig. 1.4.

Specimen Characterization

For fission-gas release the most pertinent characteristic is true surface area. A BET low-pressure, gas-adsorption apparatus (see Sec. 2.1) was built for making measurements of this type. A slight modification to

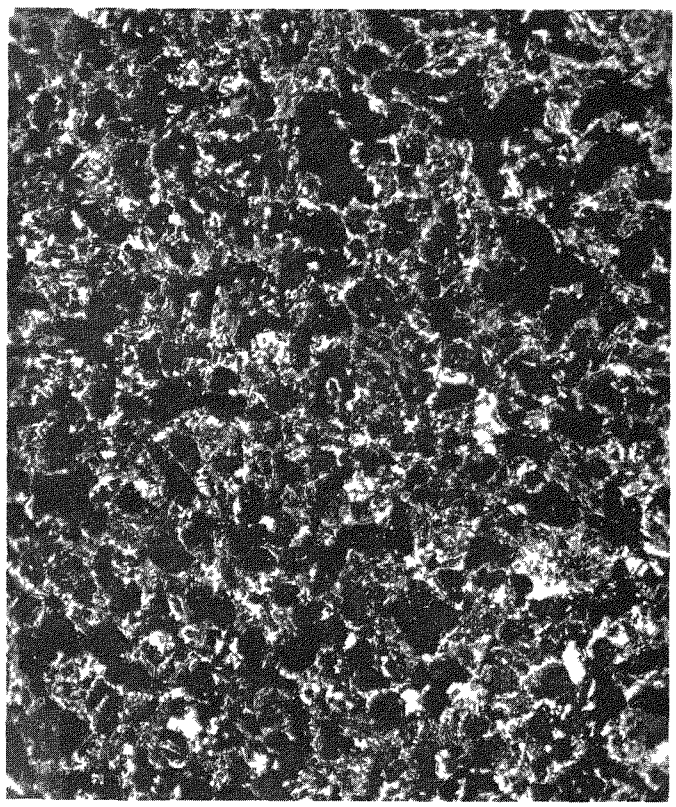

M-6020-1-1 (150×)

Fig. 1.4--Typical uniform open-type pore structure obtained in specimens of 70 UC – 30 ZrC composition prepared from narrow powder fractions (-65μ/+20μ) (Specimen No. 1066, isostatically pressed and sintered)

standard procedures is employed, in that the low surface area of the carbide specimens, relative to the fine powders normally measured by this technique, have necessitated the utilization of krypton as the adsorbing gas rather than nitrogen. Measurements are still made at liquid-nitrogen temperature.

To test the apparatus, measurements were made on the specimens listed in Table 1.3.

Table 1.3

SPECIMENS MEASURED WITH BET GAS-ADSORPTION APPARATUS

Specimen No.	Composition (mol-%)	% T. D.	Powder Size Used in Preparation of Specimen (microns)	Roughness Factor*
1055I	90 UC – 10 ZrC	81	-45	~580
1004	90 UC – 10 ZrC	90	-45	~110
1066	70 UC – 30 ZrC	79	-65/+20	~700
20T-3	30 UC – 70 ZrC	81.2	-45	~700

*Roughness factor is the ratio of true surface area to geometric area.

The plots of krypton adsorption versus relative pressure, p/p_0, (where p is the equilibrium pressure of krypton in the vapor phase for a given amount of adsorption and p_0 is the vapor pressure of krytpon at the boiling point of liquid nitrogen) are given in Figs. 1.5, 1.6, 1.7 and 1.8. Figure 1.9 is a plot of the pore size distribution, obtained by mercury porosimetry, in specimen 20T-3A (81.2% theoretical density, T. D.; 30 UC – 70 ZrC), which was a section cut from the same sample from which 20T-3 (see Table 1.3) was obtained. The plot shows the pore size to be mostly 1μ or less in size assuming the wetting angle of the mercury and carbide to be 140°. All facets of these measurements appear acceptable, and these techniques will be used to assist in the characterization of the fuel bodies used for future property measurements which are dependent upon pore distribution.

1.1.3. Control of Carbon Content in Finished UC-ZrC Specimens

Previous work at General Atomic has shown that the carbon content of hyperstoichiometric UC-ZrC can be reduced by heating specimens in the presence of flowing H_2 at ~1800°C. In order to increase the carbon

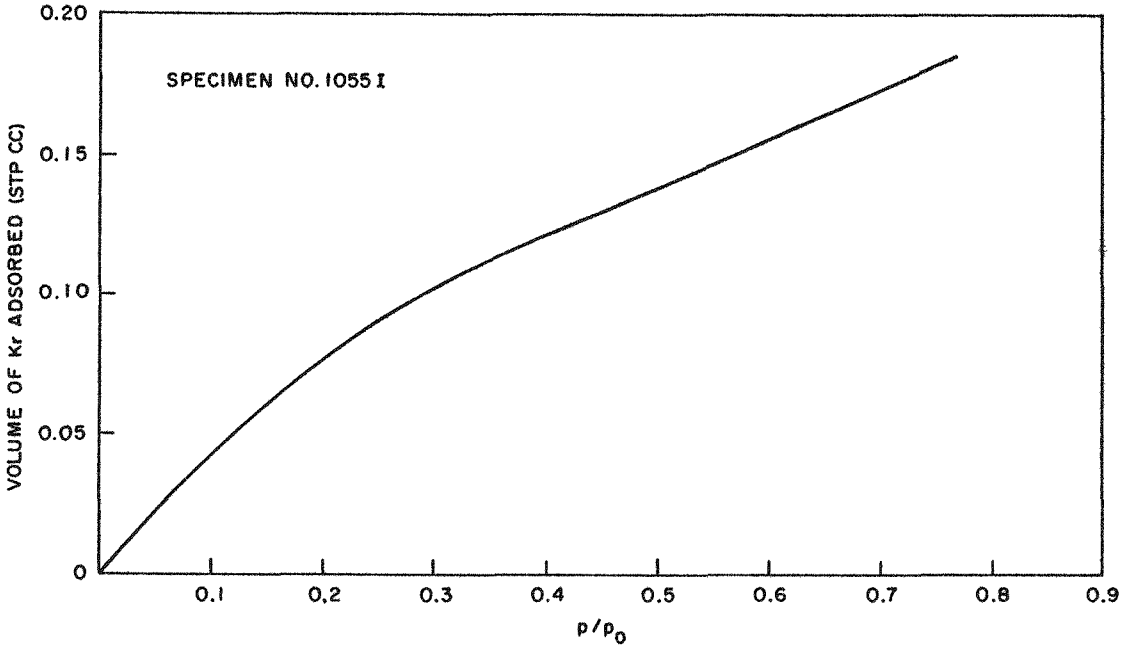

Fig. 1.5--Low-pressure krypton adsorption plot for a cold-pressed and sintered 90 UC – 10 ZrC sample of 81% theoretical density at the boiling point of liquid nitrogen

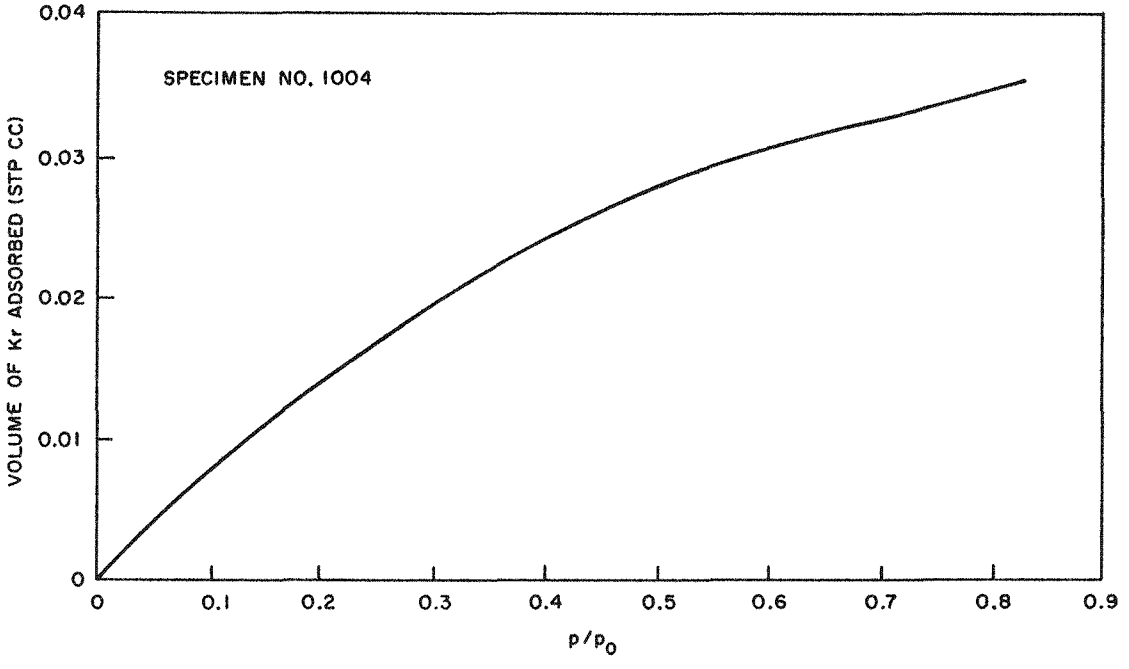

Fig. 1.6--Low-pressure krypton adsorption plot for a cold-pressed 90 UC – 10 ZrC sample of 90% theoretical density

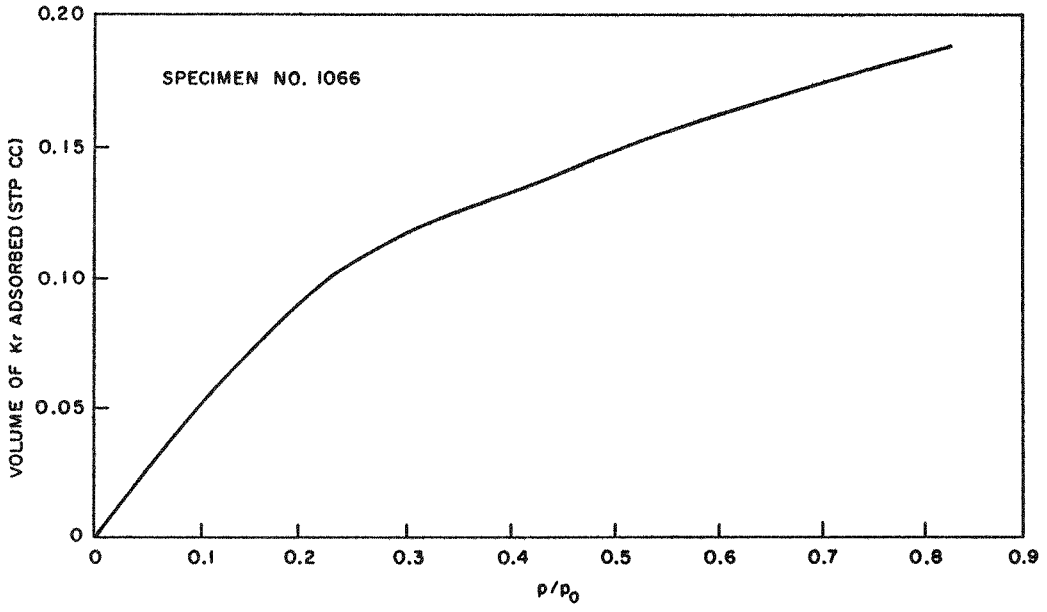

Fig. 1.7--Low-pressure krypton adsorption plot for isostatically pressed 70 UC – 30 ZrC sample of 79% theoretical density (-65μ/+20μ powder)

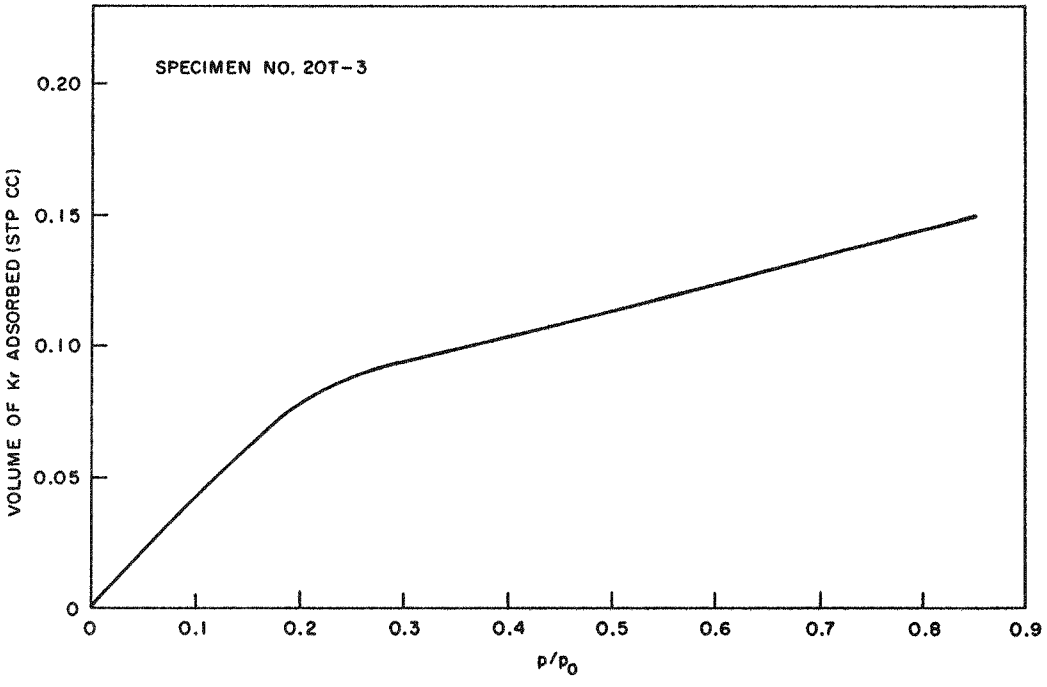

Fig. 1.8--Low-pressure krypton adsorption plot for isostatically pressed 30 UC – 70 ZrC sample of 81.2% theoretical density

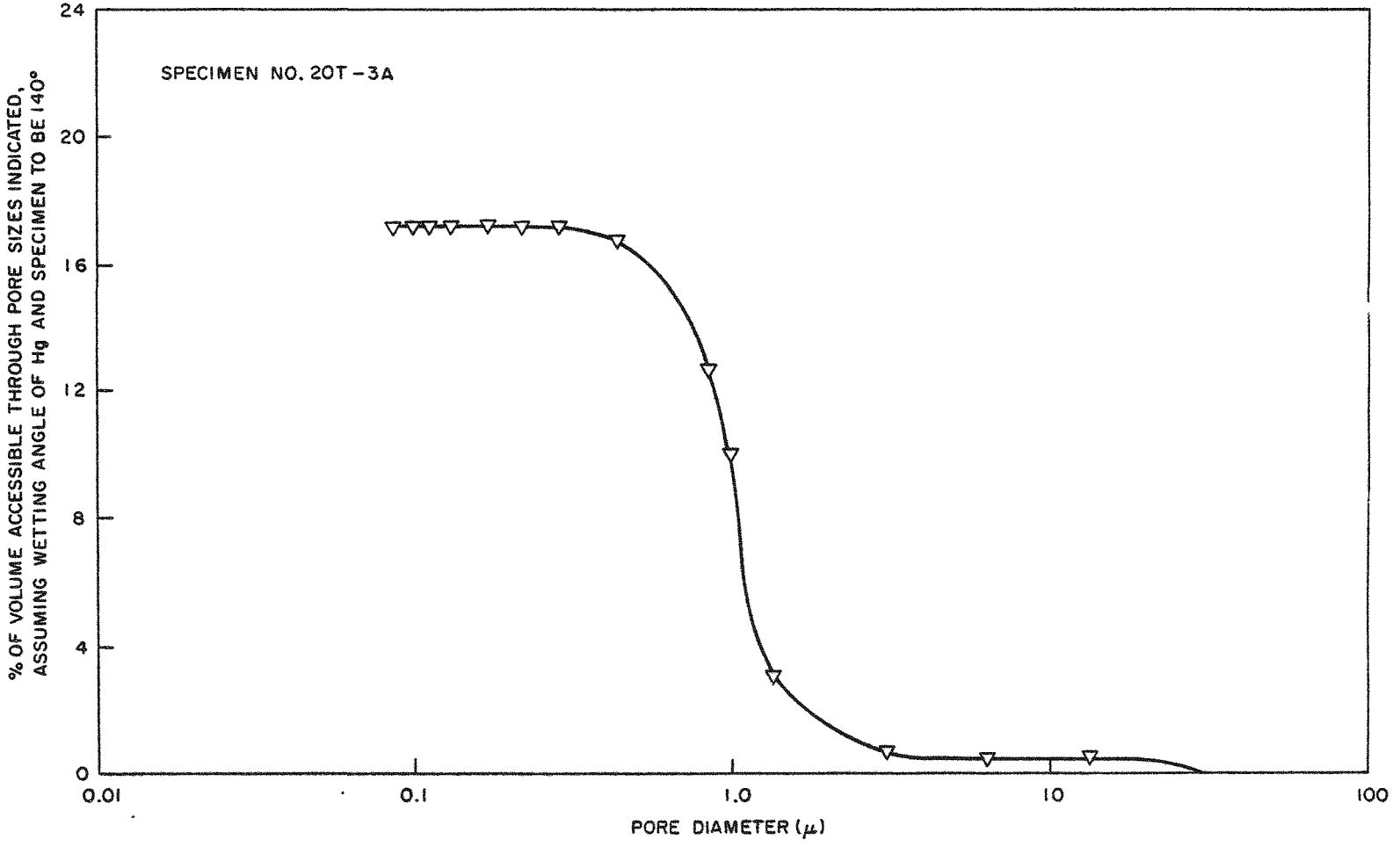

Fig. 1.9--Mercury porosimetry plot on isostatically pressed 30 UC – 70 ZrC sample of 81.2% theoretical density

content in carbide specimens, it was thought that a possible method would be to pass a mixture of H_2 and a hydrocarbon vapor over a UC-ZrC specimen at ~1800°C. This method was tried by heating two 80 UC – 20 ZrC specimens for 15 hr at 1700° to 1800°C in a gas mixture formed by passing H_2 at one atm at a rate of 2 ft^3/hr through n-heptane maintained at 25°C.

Metallographic examination of one specimen showed that a fine substructure was formed at the 1800°C end of the specimen. At the 1700°C end of the specimen a new phase was formed at the surface, and during cooling some of this "case" spalled off. Identification of this phase has not yet been accomplished. Chemical analysis indicated a decrease, rather than an increase, in the carbon content on both ends of the specimen, the decrease being larger at the 1800°C end. This probably means that the hydrogen content of the gas mixture was too high and a lower H_2 to hydrocarbon ratio will have to be tried. No oxidation was evident in the specimen, showing that the gases used were quite pure. Microprobe analysis performed on the specimen to identify the change in structure has yielded inconclusive results.

1.1.4. Gas–Metal Reaction Method for Producing Stoichiometric Carbides

This portion of the work is a continuation of work started during the last contract period and is being prosecuted to determine whether gas–metal reactions rather than arc-melting and grinding operations can be used to produce high-quality UC-ZrC powders.

A batch of 30 UC – 70 ZrC which had been prepared by hydriding and reaction with methane previously (but did not result in stoichiometric carbon content), was ground to -325 mesh and reacted with methane in the shaker furnace at 980°C for another 6 hr. A trap was used to remove hydrogen from the reaction tube. Chemical analysis of the resulting powder (which did not sinter during reaction) showed that the carbon content was 7.8 to 8.2 wt-% carbon. A specimen pressed from the material when examined metallographically appeared to be single-phase UC-ZrC. The above demonstrates that the gas–metal reaction method is amenable to producing essentially stoichiometric carbides even for high-ZrC-containing UC-ZrC materials.

1.2. DEVELOPMENT OF VAPOR-DEPOSITED TUNGSTEN TECHNOLOGY

During the last contract period the usefulness of vapor-deposited tungsten for high-temperature nuclear applications was amply demonstrated. It is now necessary not only to utilize this material but also to understand its characteristics and learn how to control them.

In all of our studies to date it has become apparent that on a fine scale

the process, as commercially available, is not providing a reproducible product. Of course, defining reproducibility itself is a difficult problem, whether it be the chemistry, microstructure, strength (at high or low temperature), ductile-to-brittle transition temperature, or thermionic emission. It is apparent that the definition must itself be related to the application. However, in some fashion the reproducibility must be demonstrated and controlled before too much effort is expended on the measurements of properties of irreproducible samples. The question of reproducibility is therefore the main problem to which attention is being directed. In addition, some effort is also being focused towards the solution of immediate problems with respect to the fabrication of irradiation specimens, viz., the coating of fuels and the inhibition of grain growth. Work is progressing by two means:

First, the capability of making vapor-deposited tungsten under carefully controlled conditions is being obtained at General Atomic. R. A. Holzl of San Fernando Laboratories has consented to act as a consultant.

Second, a research and development subcontract is being negotiated with San Fernando Laboratories to conduct work at their site.

The development of deposition capabilities at General Atomic has two initial phases:

1. To obtain reproducibility of deposits through careful control of all operative variables.

2. Using one set of deposition conditions as a base line, to conduct experiments with minor perturbations in operational parameters. The changes will be of the order of magnitude one might expect from a lack of precise control of the process; i.e., large changes will not be employed in order to determine properties over a vast range of variables, but rather, small changes on the order of those which could occur during a run will be studied. The purpose is to determine which are the most important variables to control and to allow the setting of reasonable specifications for future hardware work. Variables which will be studied are

   a. Temperature

   b. Flow rate

   c. Gas mixture

   d. Purity of starting materials, WF_6, H_2, and any other gases employed

   e. Substrate surface: both material and surface preparation

f. Gross-contamination from structural components of system

g. Cleanliness of system

The assembly of the apparatus to be used in this portion of the program is nearing completion. A schematic diagram of the apparatus is shown in Fig. 1.10. The initial form of deposits will be tubes on the order of 1/2 in. ID by 1-1/2 in. long. All materials of construction have been selected to eliminate or at least to minimize the contamination of reactants through chemical interactions. As soon as construction of the apparatus is completed (estimated, January 15, 1964) experimentation will be initiated.

The program at San Fernando Laboratories will consist of the following:

1. To study in greater detail than previously the relationship between the compatibility of reactor fuels and plating conditions.

2. To study the protection afforded fuels by thin, vapor-deposited tungsten seal coats. (These seal coats are deposited under conditions such that the interactions between the fuel and the gaseous reaction products of the deposition process are minimized; see Sec. V of Ref. 1.) This will include items such as the thickness required (and its relation to the plating conditions used) to provide protection against HF at elevated temperatures. This test was selected since HF is the reaction product primarily responsible for attack of carbides and oxides during deposition.

3. To provide coated samples to our laboratory for evaluation of their thermal stability.

4. To provide specimens to our laboratory which shall be jointly designed to allow studies of the effect of high-angle grain boundaries, contamination, and cold-work on the grain-growth characteristics of vapor-deposited tungsten.

5. To study the inhibition of grain growth by interruptions during plating and to determine the characteristics required by such interruptions. Evaluation of the specimens prepared will be performed by General Atomic.

Negotiations of the contract to perform this program are in progress.

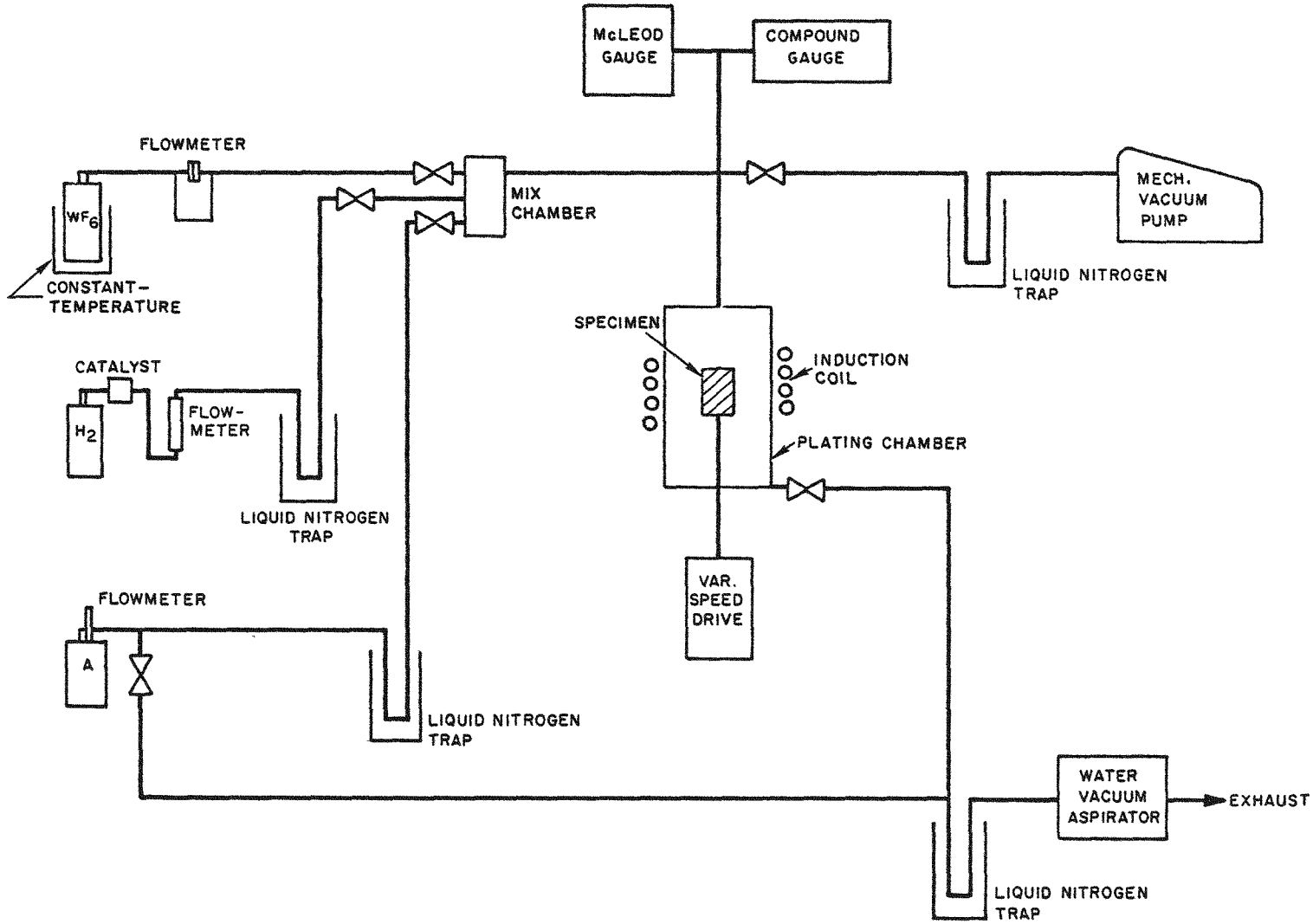

Fig. 1.10--Schematic diagram of tungsten vapor-plating apparatus

Section II

MEASUREMENTS OF HIGH-TEMPERATURE PROPERTIES OF THERMIONIC MATERIALS

The objective of the measurements made under this section of the program are twofold: to improve our understanding of the physical and mechanical properties of the UC-ZrC and the vapor-deposited tungsten-clad fuel systems for thermionic applications, and to study other refractory metal-fuel system and emitter concepts as possible thermionic cathode candidates. The sample coding system is shown in Table 2.1.

Table 2.1

CODING SYSTEM FOR SAMPLES USED IN THE MEASUREMENT OF HIGH-TEMPERATURE PROPERTIES OF THERMIONIC MATERIALS

Task	Sample
2.1 Rate of vaporization of UC-ZrC as a function of pore structure	A_1(1, 2, 3, ---)*
2.2 Fission-product release from UC-ZrC	A_2(1, 2, 3, ---)
2.3 Fission-product diffusion through tungsten clad	A_3(1, 2, 3, ---)
	A_4(1, 2, 3, ---)

2.4 Fuel-emitter gross diffusion	D_1(1, 2, 3, ---)†
	D_2(1, 2, 3, ---)

2.5 Fuel-emitter diffusion-emission	E_1, E_2, E_3, ---
2.6 Refractory metal interdiffusion	F_1(1, 2, 3, ---)†
	F_2(1, 2, 3, ---)

2.7 Refractory metal diffusion-emission	G_1, G_2, G_3, ---
2.8 Mechanical properties of UC-ZrC	H_1, H_2, H_3, ---
2.9 Emission microscopy of uranium-containing tungsten cermets	I_1, I_2, I_3, ---

*Number in parentheses refers to sections cut from the same sample.

†Number in parentheses refers to samples included in the same diffusion run.

2.1. RATE OF VAPORIZATION OF UC-ZrC AS A FUNCTION OF PORE STRUCTURES

Previously,[1] it has been shown that UC-ZrC samples containing large numbers of open pores vaporize at a higher rate than those containing fewer open pores. The purpose of the work reported in this section is to try to characterize the pore structures of UC-ZrC samples by measuring their true surface area by the Brunauer-Emmett-Teller (BET) gas-adsorption method[5] and their pore-size distribution by the mercury porosimeter technique. Correlation will be sought between the surface roughness factor R (defined as the ratio of true surface area to geometrical surface area of the sample), the pore-size distribution of UC-ZrC samples, and their Langmuir rates of vaporization. Slices from the same samples, used for the study of the variation of their fission-product release properties with pore structures, are discussed in Sec. 2.2, and those used as the fuel sample for the study of fission-product diffusion through tungsten clad are discussed in Sec. 2.3.

To determine the true surface area of UC-ZrC samples, a BET low-pressure adsorption apparatus has been built, utilizing krypton gas at the boiling point of liquid nitrogen. Figure 2.1 shows the arrangement of such an apparatus. The carbide sample is contained in a glass sample chamber, the dead volume of which is reduced to a minimum by using glass spacers. The sample is baked at 450°C in vacuum ($\sim 10^{-6}$ torr) overnight before krypton is introduced into the system at a known pressure and the sample chamber is immersed in liquid nitrogen. After equilibrium is reached, the change in the krypton pressure in the system due to adsorption is measured with a McLeod gauge, from which the volume V (reduced to 0° and 1 atm) of krypton adsorbed is deduced. The experiment is repeated for a number of starting krypton pressures and the values of V obtained are plotted against the relative pressure p/p_0, where p is the equilibrium pressure of krypton in the vapor phase for a given amount of adsorption and p_0 is the vapor pressure of krypton at the boiling point of liquid nitrogen ($\sim$1.78 torr). The point where the curve changes to a straight line corresponds to monolayer adsorption. From the volume of krypton (0°C and 1 atm) for monolayer adsorption on the sample surface and the conversion factor 10^{15} Kr atom/1 cm^2, the total surface area of the sample can be calculated. Typical BET adsorption curves have been shown in Sec. I of this report. The first sample studied in this section, A_1, is a hot-pressed, 10%-enriched 30 UC – 70 ZrC sample of high density ($\sim$97% theoretical density). A_1 was cavitroned to form circular pieces of 3/8-in. diameter. The first piece, A_1-1 (1/8-in. thick), was used for the study of the vacuum vaporization rate. The results obtained are shown in Table 2.2 and are plotted in Fig. 2.2. The true surface area of the sample, however, is too small to be measured even by krypton low-pressure adsorption. An ethane (C_2H_6) source is being added to the BET apparatus. This source, because

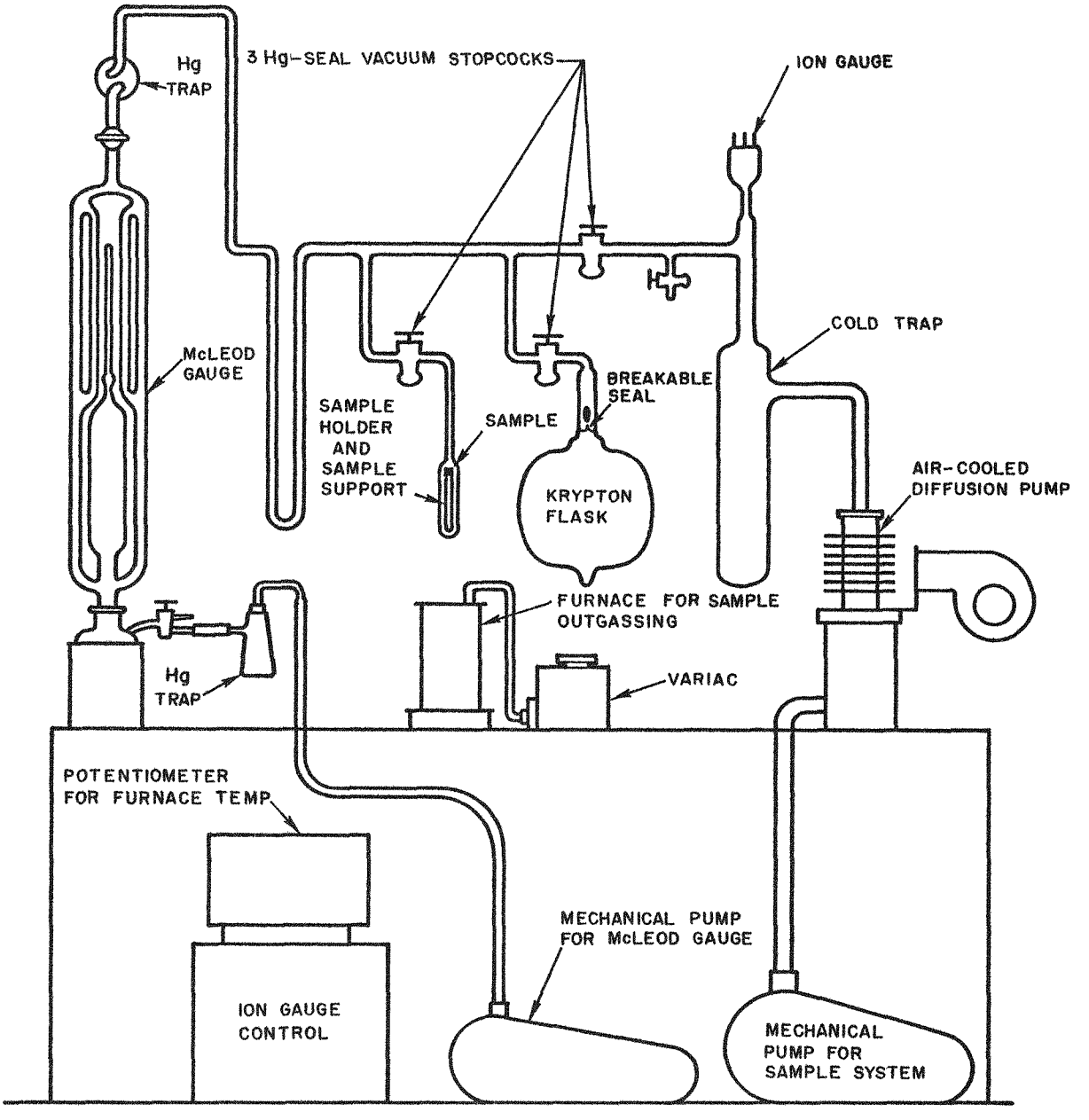

Fig. 2.1--BET low-pressure adsorption apparatus

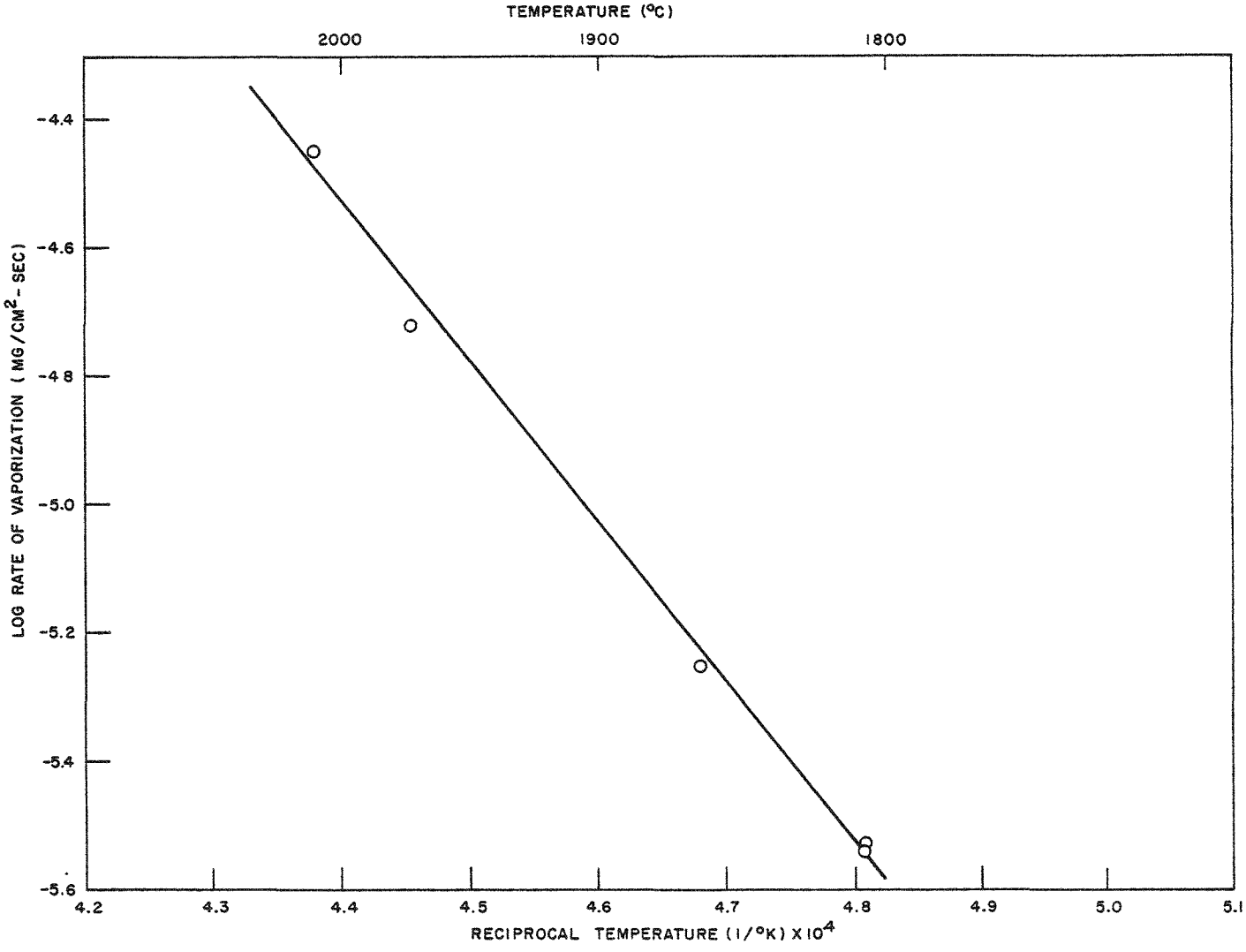

Fig. 2.2--Log rate of vaporization versus reciprocal temperature for sample A_1-1 (hot-pressed 30 UC – 70 ZrC sample)

of its lower vapor pressure at liquid nitrogen temperature than that of krypton, may be used for determining very small surface areas. Mercury-porosimeter study and microstructure examination will follow the ethane adsorption study. Three other samples, A_2, A_3, and A_4, which are cold-pressed and sintered 30 UC – 70 ZrC samples of 77%, 84%, and 91% theoretical density, respectively, have been prepared for these studies.

Table 2.2

VACUUM VAPORIZATION STUDIES OF SAMPLE A_1-1*
(30 UC – 70 ZrC, hot-pressed)

Run No.	Temp. (°K)	Exposure Time (sec × 10^5)	Rate of Weight Loss (mg/cm^2-sec × 10^{-5})	Density (g/cm^3)
Original	----	----	----	8.83
Degas	2150	1.983	2.10	8.77
1	2283	0.288	3.59	8.77
2	2245	1.404	1.91	8.76
3	2080	0.936	0.294	8.76
4	2141	0.756	0.561	8.80
5	2080	1.080	0.283	8.80

*Sample was hot-pressed at approximately 7000 psi at 1800°C. Final composition, porosity, and BET surface area to be determined.

2.2. FISSION-PRODUCT RELEASE FROM UC-ZrC

The purpose of the study is to correlate the rates of release of fission products from UC-ZrC fuels of various compositions with their surface roughness factors and pore-size distribution in the temperate range of 1600°C to 2000°C. The results should help to guide the selection of fuel materials and their fabrication techniques for the irradiation studies and for in-pile cesium cell applications. The method used is the postirradiation annealing type in which the fuel samples are irradiated at ambient temperatures to a known number of fissions. After a suitable cooling-off period, the sample is quickly brought to the temperature planned, and the release of the fission products Xe^{133}, Ba^{140}, Te^{132}, and I^{131} is determined as a function of annealing time. These particular nuclides were selected for the study because they are of adequate yield and of convenient half-life for postirradiation experiments. Also, they represent three important classes of fission products: xenon, a noble gas; barium, an electropositive metallic element; and tellurium and iodine, electronegative nonmetallic elements. The rates of release of volatile fission products (especially krypton and xenon) are of particular interest, since they are closely related to the fuel swelling problem.

The general procedures for the determination of the fission-product release by the postirradiation annealing method are as follows:

The sample is irradiated in General Atomic's TRIGA reactor to about 10^{13} to 10^{14} fissions in an aluminum purge can which is leak-checked prior to the irradiation. Thus, recoil release can be measured by purging the Xe^{133} released into the can before the high-temperature annealing treatment. Usually the irradiated sample is cooled for about 5 days to allow the Xe^{133} to grow in. The annealing of the sample is carried out in a King furnace, which is essentially a resistance-heated graphite tube supported in a helium atmosphere (see Fig. 2.3). A helium purge is used to sweep the released Xe^{133} to a remote liquid-nitrogen-cooled charcoal trap, where it is collected and continuously monitored with a scintillation detector. A cold finger extends down the center to within an inch of the sample and collects the released I^{131} and Te^{132}. The inside of the heater tube is lined with a tantalum diffusion barrier which channels the volatile fission products downstream and prevents diffusion through the walls of the heater tube (see Fig. 2.4). The UC-ZrC samples are placed in a tungsten sleeve to prevent contact and thus reaction with graphite. The tungsten sleeve, in turn, is placed in a removable graphite sleeve which serves as a collector for Ba^{140}. This sleeve is changed and the cold finger is sampled as frequently as possible in order to obtain release rate data for I^{131}, Te^{132}, and Ba^{140}. By measuring the 1.60-Mev peak of La^{140} in the irradiated sample, an accurate estimate of the number of fissions is obtained and from fission-yield data the quantity of any fission product initially present can be calculated.

Three samples have been studied during this reporting period. These are A_1-2, A_1-3, and A_1-4, which were cut from the same hot-pressed high-density (96% theoretical density) 30 UC – 70 ZrC piece as sample A_1-1 which has been studied for its vaporization rates (see Sec. 2.1). All three samples are in the form of thin disks (0.38-in. diam, 0.06 in. thick) and have been outgassed in vacuum at 1900°C for a period of 22 hr. They were stored in helium prior to irradiation. Sample A_1-2 was irradiated to 6×10^{13} fissions and studied at 1800°C, while sample A_1-3 was irradiated to 1.2×10^{14} fissions and studied at 1900°C. The results obtained on sample A_1-4 (1.2×10^{14} fissions, 1800°C) are abnormally high, probably due to surface oxidation of the sample, and therefore are not included here. To avoid thermal shock, all samples were brought to temperature over a period of 1/2 hr.

Figures 2.5 and 2.6 are the plots of the results of samples A_1-2 and A_1-3, shown in Table 2.3. The final fractional release rates calculated from the slope at the final point of the linear plot of fractional release versus time are listed in Table 2.4. Each of the curves shown in Figs. 2.5 and 2.6 exhibits an initial portion of rapid release, followed by another

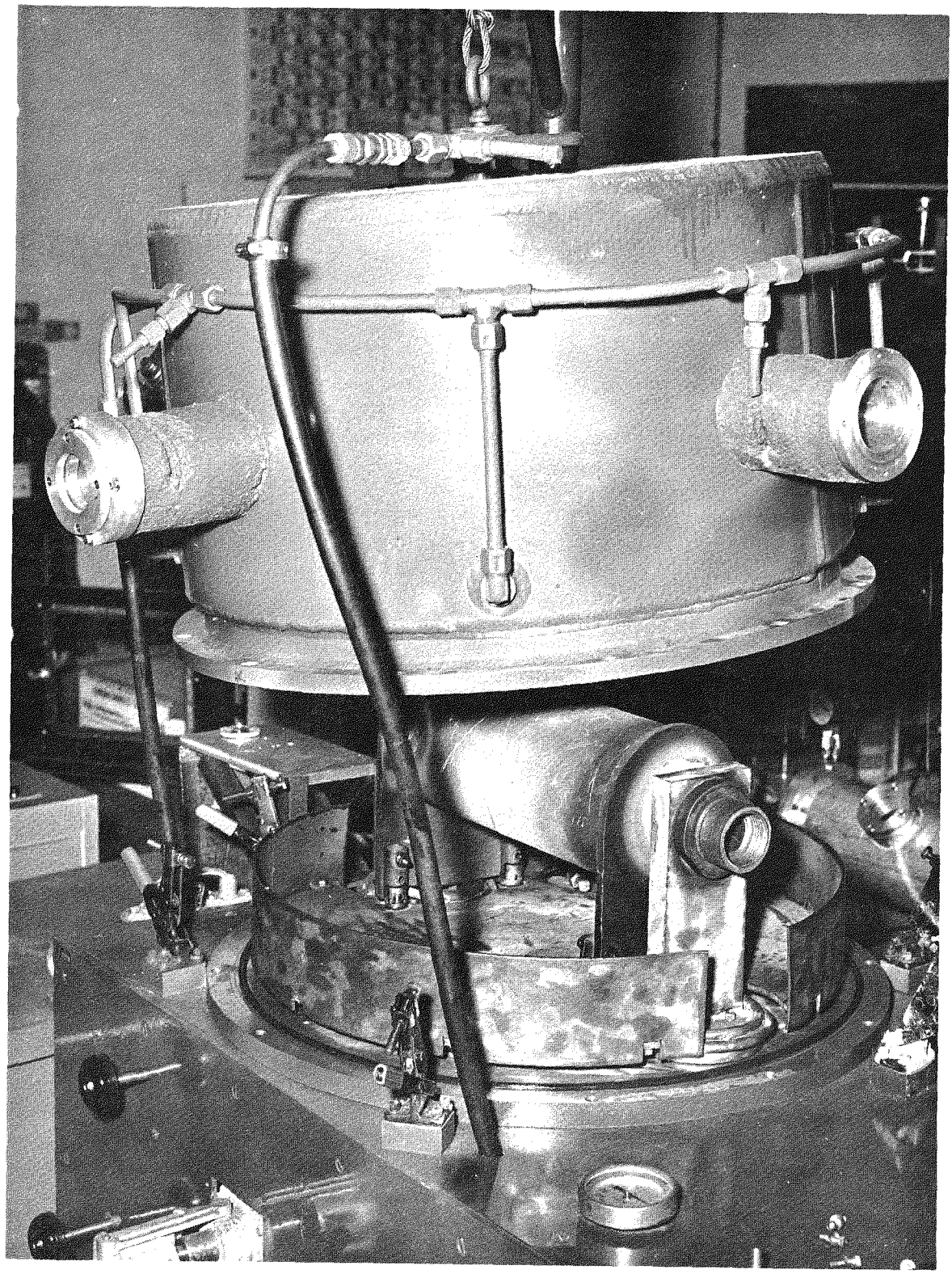

HT-11004

Fig. 2.3--King furnace used for the postirradiation annealing studies of fission-product release from UC-ZrC

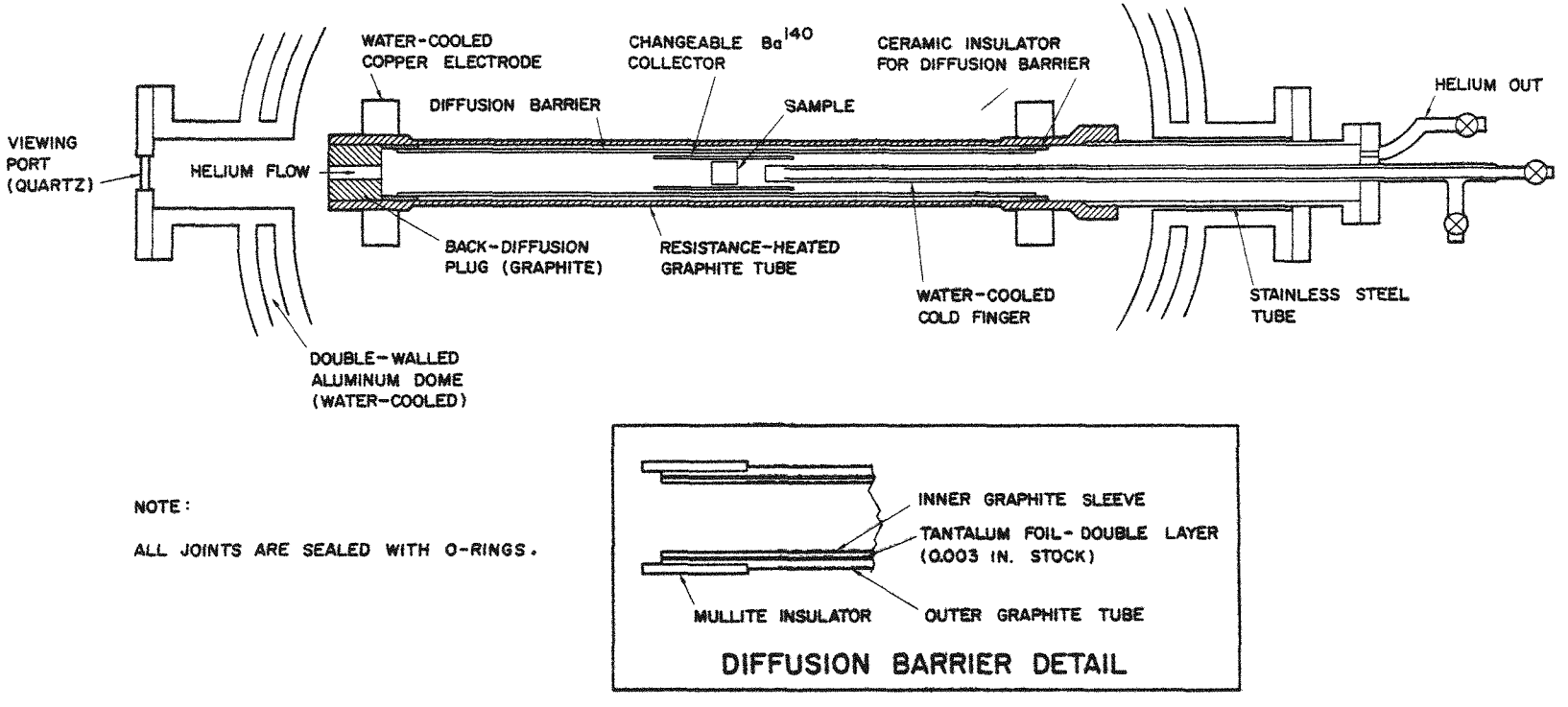

Fig. 2.4--Top view of the arrangements in the King furnace

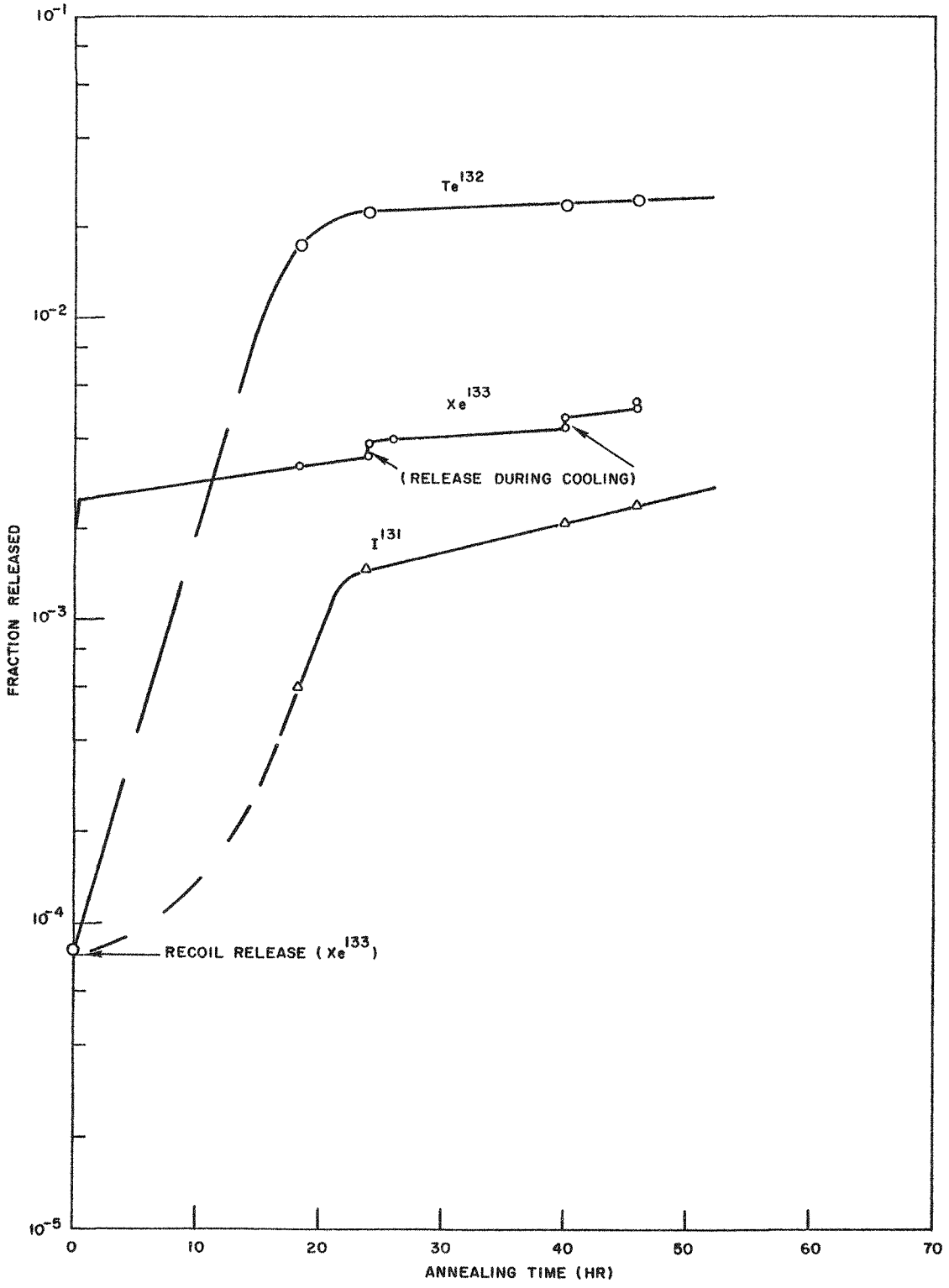

Fig. 2.5--Fission-product release at 1800°C for 97%-dense 30 UC – 70 ZrC (sample A_1-2)

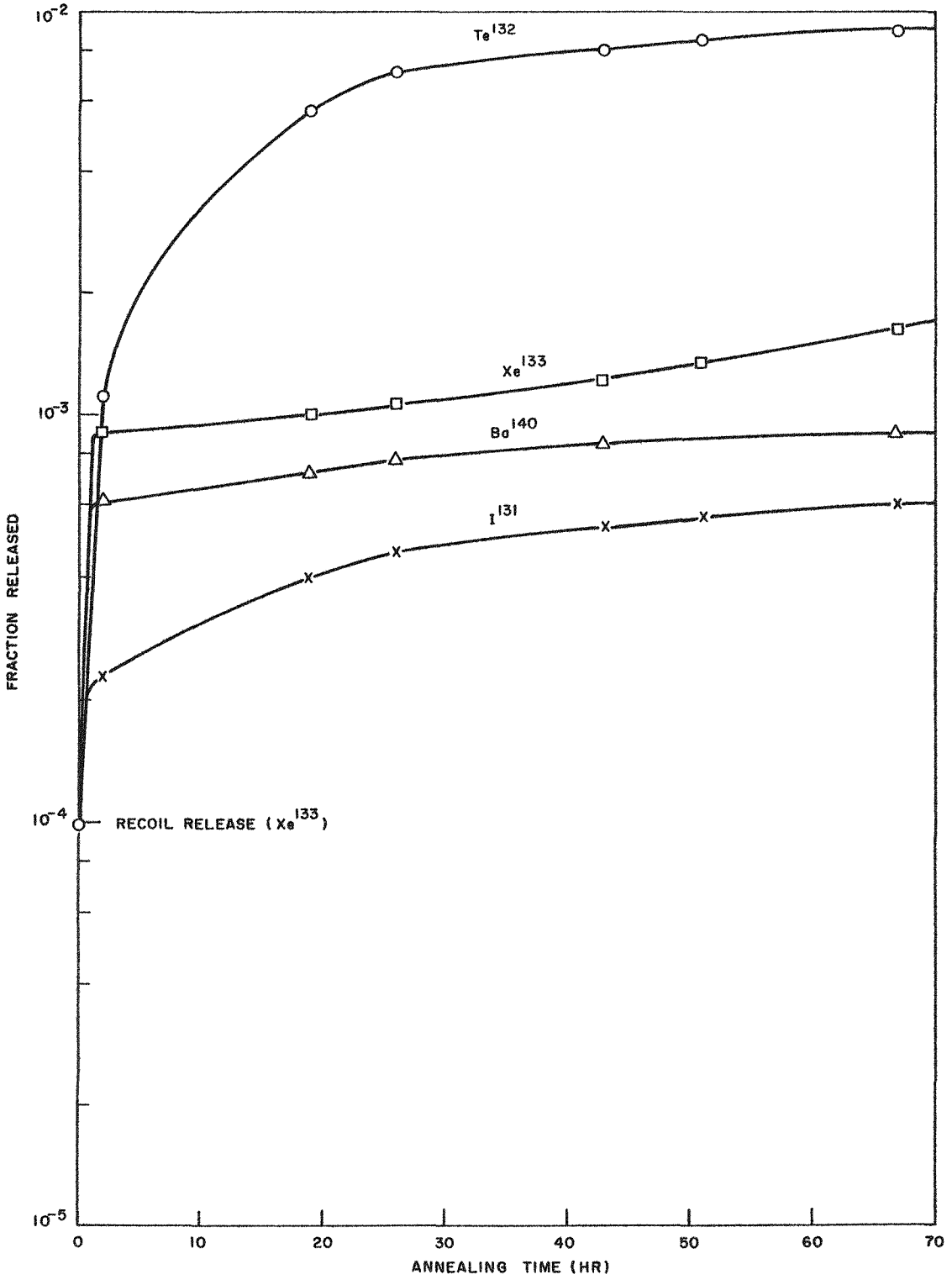

Fig. 2.6--Fission-product release at 1900°C for 97%-dense 30 UC – 70 ZrC (sample A_1-3)

Table 2.3

FISSION-PRODUCT RELEASE FROM 30 UC – 70 ZrC IN ANNEALING RUNS

Sample No.	Temp. (°C)	Time (hr)	Fraction Released			
			Xe^{133}	Te^{132}	I^{131}	Ba^{140}
A_1-2	1800	0 (recoil)	7.9×10^{-5}	-----	-----	-----
		18.5	3.2×10^{-3}	1.8×10^{-2}	5.9×10^{-4}	-----
		24	3.4×10^{-3}	-----	-----	-----
		(After cooling)	3.8×10^{-3}	2.2×10^{-2}	1.4×10^{-3}	-----
		40.5	4.2×10^{-3}	-----	-----	-----
		(After cooling)	4.6×10^{-3}	2.4×10^{-3}	2.0×10^{-3}	-----
		46.5	4.9×10^{-3}	-----	-----	-----
		(After cooling)	5.2×10^{-3}	2.5×10^{-2}	2.3×10^{-3}	2.0×10^{-3}
A_1-3	1900	0 (recoil)	9.8×10^{-5}	-----	-----	-----
		2	8.9×10^{-4}	1.2×10^{-3}	2.3×10^{-4}	6.0×10^{-4}
		19	9.9×10^{-4}	5.6×10^{-3}	3.9×10^{-4}	7.1×10^{-4}
		26	1.1×10^{-3}	7.0×10^{-3}	4.6×10^{-4}	7.7×10^{-4}
		43	1.2×10^{-3}	7.9×10^{-3}	5.2×10^{-4}	8.4×10^{-4}
		51	1.3×10^{-3}	8.5×10^{-3}	5.6×10^{-4}	-----
		67	1.6×10^{-3}	8.9×10^{-3}	6.0×10^{-4}	9.1×10^{-4}

Table 2.4

FINAL RELEASE RATES*

Sample No.	Temp. (°C)	Xe^{133}	Te^{132}	I^{131}	Ba^{140}
A_1-2	1800	2.0×10^{-5}	1.0×10^{-4}	4.4×10^{-5}	-----
A_1-3	1900	1.8×10^{-5}	2.5×10^{-5}	2.3×10^{-6}	2.9×10^{-6}

*Fractional release per hour.

portion of much slower release rates. As seen from Fig. 2.5, the Xe^{133} release from sample A_1-2 shows a sensitivity to thermal cycling. Small bursts of Xe^{133} release occurred each time that the furnace was cooled for the collection of the condensate on the cold finger; the first burst was missed when trapping was temporarily interrupted. It is possible that microcracks might have occurred in the sample upon cooling (1800° to 500°C in 10 min and 500°C to room temperature in 20 min), which facilitated the release. Radiochemical analyses performed on sample A_1-2 showed that the retention of Mo^{99}, Ce^{141}, and Cs^{137} was virtually 100%.

Sample A_1-3, which was studied at 1900°C, gave lower release rates (see Table 2.4) than that of sample A_1-2, which was studied at 1800°C. This appears to be anomalous, since release rates, in general, are expected to increase with temperature. It is possible that the higher release rates of sample A_1-2 are due to the presence of defects in sample A_1-2. It is interesting to note that there was no thermal-cycling effect with sample A_1-3. It appears that additional experiments are needed to clarify the anomalous observations of lower release rates at 1900°C than at 1800°C and to obtain data over a range of temperatures so as to establish activation energies for the fission-product release process.

2.3. FISSION-PRODUCT DIFFUSION THROUGH TUNGSTEN CLADDING

The purpose of the study is to determine the rates of diffusion of various fission products from uranium-containing fuels through tungsten cladding in the temperature range 1600°C to 2000°C as a function of the structures of the tungsten cladding. The experiment will be performed in an arrangement similar to the diffusion-emission cell, the details of which have been described in the final report of Contract NAS 3-2532.[1] The fission gases diffusing through the cladding will be caught in a liquid-nitrogen-cooled charcoal trap and monitored in situ. The other fission products diffusing through the clad will be condensed on a water-cooled copper surface coated with carbon. The carbon coating is used to facilitate the capture of strong carbide-forming fission products. During the experiment, the vacuum emission of the tungsten surface will be monitored for any change. The results should indicate how clean the tungsten surface and the cesium plasma can be kept during the operation of a tungsten-clad emitter in a reactor. The correlation of the rates of diffusion with structures of the tungsten cladding should serve as a guide for the selection of optimum fabrication methods.

Figure 2.7 shows the experiment arrangements used and is self-explanatory. Fabrication of one of the cells has been completed, and the pulse-height analyzer has been ordered. The first sample to be studied will be a vapor-deposited tungsten-clad, low-density 30 UC – 70 ZrC cut

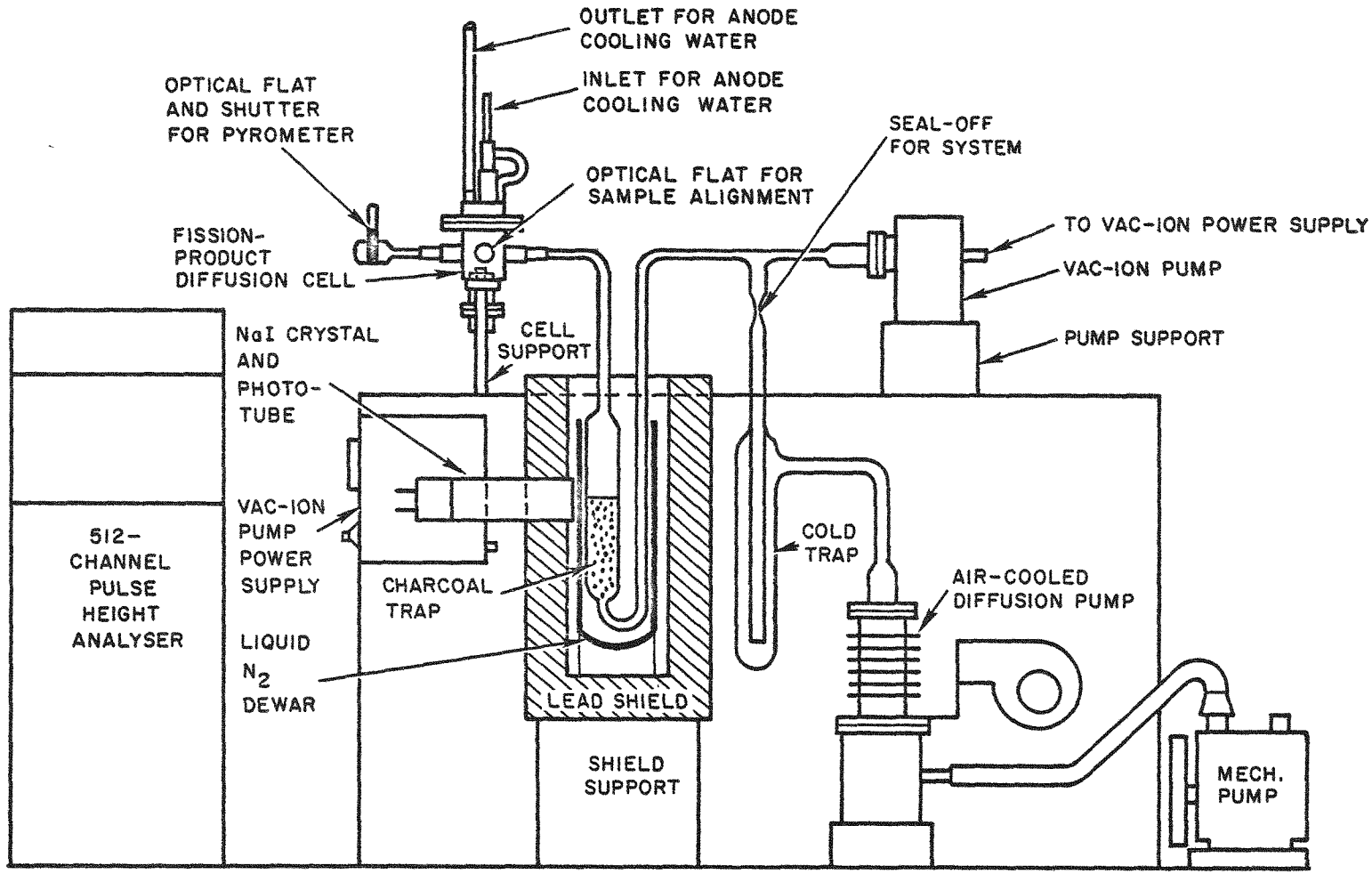

Fig. 2.7--Experimental arrangements for the study of fission-product diffusion through tungsten clad

from the carbide cylinder A_2 (see Sec. 2.1). The use of a low-density fuel sample will insure that the release of fission products from the fuel itself is not the rate-determining step of the over-all process, so that some preliminary ideas may be gained on the rates of diffusion of various fission products through the cladding.

2.4. GROSS DIFFUSION STUDIES OF FUEL-CLAD SYSTEMS

Previous diffusion studies[1][2] have been made on a number of emitter-fuel combinations, mostly at 1800°C, and utilizing uranium-containing fuels (e.g., UC, UC_2, UC-ZrC, and UO_2) coupled to specific refractory metals and alloys (e.g., W, Ta, Mo, Nb, Ir, Re, W-25Re, W-15Mo, and W-2Mo). These screening experiments revealed several promising fuel-clad systems. Also, various types of interaction between the fuels and refractory metals were observed and detected. A continuation of this study has been planned to broaden the information concerning the limits of temperature and compositions for which specific clad-fuel combinations can be successfully utilized. Of particular interest is the temperature region of 1400°C to 2000°C for periods of time up to 1000 hr.

A summary of the compatibility results between various fuel–refractory-metal-clad systems is given in Table 2.5. Also included are the compatibility properties of certain fuel-clad combinations, which are deduced from the results of some prior experiments. In view of the large number of fuel-metal combinations to be examined over a range of temperatures, critical experiments have been planned in order to reduce the portion of fuel composition-temperature spectrum to be studied; this sequence of the first seven experiments is listed in Table 2.5. The first several experiments will begin with UC-ZrC of low uranium content, i.e., 30 UC – 70 ZrC.

During this first quarter, high-purity refractory metals were procured, and various uranium-fueled compounds needed were prepared. Since the stoichiometry of the fuel bodies may be one of the important factors affecting the results, each fuel sample must be prepared under careful conditions. Fuel samples will be studied at both stoichiometric and slightly hyperstoichiometric compositions. The chemical compositions and metallography for all of the refractory metals have been checked and recorded. The chemical analysis and metallography of each specific fuel composition will be recorded just prior to each experiment. This has been accomplished for the 30 UC – 70 ZrC specimens for the first five experiments.

Other activities have included the modification and rebuilding of the present diffusion furnace. This was accomplished and the furnace has been tested at 2000°C at a residual gas pressure of 10^{-6} torr. Also, because of

Table 2.5

COMPATIBILITY OF VARIOUS FUELS AND REFRACTORY METALS AS DETERMINED BY GROSS-DIFFUSION EXPERIMENTS AT VARIOUS EXPERIMENTAL TEMPERATURES FOR 50 HR

The experimental temperatures are in °C. Suitable combinations at specific experimental temperatures are indicated by YES, unsuitable combinations by NO, and questionable combinations by ?. Parentheses around the YES, NO, or ? indicate a judgment by deduction. The numbers indicate the planned sequence of further experiments.

Refractory Metal	UC				90 UC – 10 ZrC				50 UC – 50 ZrC				30 UC – 70 ZrC				10 UC – 90 ZrC				UC_2				UO_2			
	1400	1600	1800	2000	1400	1600	1800	2000	1400	1600	1800	2000	1400	1600	1800	2000	1400	1600	1800	2000	1400	1600	1800	2000	1400	1600	1800	2000
Tungsten	(Yes)	(Yes)	Yes	6	(Yes)	(Yes)	Yes	6	(Yes)	(Yes)	(Yes)	6	(Yes)	(Yes)	Yes	6	(Yes)	(Yes)	Yes	6			No[b]	(No)	(Yes)	(Yes)	Yes	Yes
Molybdenum			No[a]	(No)			No[a]	(No)					4	2	1		(Yes)	(Yes)	Yes				No[b]	(No)		7	No[d]	No[d]
Niobium			No[a]	(No)			No[a]	(No)					4	2	(No)	(No)			No[c]	(No)			No[b]	(No)		7	No[d]	No[d]
Tantalum			No[a]	(No)			No[a]	(No)					4	2	(No)	(No)			No[c]	(No)			No[b]	(No)		7	No[d]	No[d]
Iridium			No[a]	(No)									5	3	1											7		
Rhenium			?										5	3	1											7		
W-25 Re			?										5	3	1											7		
W-15 Mo			No[a]	(No)																								
W-2 Mo			No[a]	(No)			No[a]	(No)							No[d]	(No)												

[a] Unsuitable because of liquid-phase formation.

[b] Unsuitable because of excessive carbide-layer formation and grain-boundary penetration.

[c] Unsuitable because the uranium and zirconium diffuse into the metal at too rapid a rate.

[d] Unsuitable because of fuel-component diffusing through the grain boundaries.

the large number of specimens required to cover the composition-temperature ranges to be studied, an additional diffusion furnace capable of holding more than one specimen was ordered. Delivery is expected by January 20, 1964.

Tantalum diffusion capsules for containment of the fuel-metal couples have been prepared, and mating surfaces of the refractory metal and fuel specimens are now being carefully aligned and polished for the first three experiments. The experiments will begin in the first month of the next quarter.

2.5. FUEL-CLAD DIFFUSION-EMISSION STUDIES

This is a continuation of the work under Contract NAS 3-2532[1] for the study of trace diffusion of fuel components into the clad by electron emission monitoring. The apparatus used has been described in the final report of Contract NAS 5-1253.[2] Previously, studies have been made[1] on vapor-deposited tungsten-clad UC (both carbon-rich and metal-rich), UO_2, and 30 UC – 70 ZrC. During this quarter, experiments have been extended to the case of rhenium-clad UC, since this fuel-clad combination has been found to be a questionable case on the basis of gross diffusion studies.[1]

The sample, E_1, was prepared by bonding a 20-mil-thick rhenium sheet to a cast tungsten cup containing a cold-pressed and sintered UC wafer (20-mil-thick, 4.63% carbon). The bonding was carried out in a vacuum hot-press at 1900°C for a period of 1-1/2 hr. To prevent the graphite plungers from reacting with the rhenium and the tungsten, a 5-mil-thick tungsten sheet was used as a spacer at the cast tungsten side, and a 20-mil W-26 Re sheet and a 5-mil tungsten sheet were used as spacers at the rhenium side, with the W-26 Re sheet facing the rhenium. After bonding, the sample was pressurized with helium and checked for the soundness of the bond by immersion in acetone. The spacer sheets were then machined off by electrical discharge machining (EDM). To insure a clean rhenium surface, the top 7 mils of the rhenium layer was also removed by EDM so that the final thickness of the rhenium clad was 13 mils.

The sample was heated in the diffusion-emission cell for 64 hr at 1923°K, 170 hr at 2063°K, 50 hr at 1663°K, and finally another 16 hr at 2063°K. The Schottky plots obtained after the sample was 1 hr, 24 hr, and 186 hr at 2063°K are shown in Fig. 2.8. It can be seen that after the sample was heated at 2063°K for only 1 hr (after 64 hr at 1923°K), the saturation emission at zero field was 30 ma/cm^2 as compared to a value of 0.4 ma/cm^2 for rhenium at the same temperature. After 24 hr at 2063°K, the emission could not be saturated because the molybdenum collector and the molybdenum guard ring, which were both "floated," i.e., not cooled, became excessively

heated due to the large current emitted from the surface of the sample. Saturation could be achieved, however, when the sample was cooled to 1663°K (after 170 hr at 2063°K). Figure 2.9 shows the variation of the vacuum-saturation emission with time at 1663°K. The emission increased with time, indicating a continuous adjustment of the surface composition by diffusion. Although a steady state was not reached after 50 hr at 1663°K, it is apparent that the saturation emission of the surface at the end of 50 hr (14 ma/cm^2) is many orders of magnitude higher than that of pure rhenium (5×10^{-4} ma/cm^2) at the same temperature.

In view of the large change of emission observed, the experiment was terminated, and the sample was sectioned and examined both metallographically and by the electron microprobe technique. Figure 2.10 shows the photomicrograph taken at the Re-UC interface. It is evident that reaction has occurred between the rhenium and the metal-rich UC and that it is difficult to locate the position of the original interface. Electron microprobe studies indicated that rhenium had penetrated into the carbide for about 100 microns (μ) (see Fig. 2.11) but no uranium (within 0.1%) was detected inside the rhenium. The rhenium-containing phase in the UC was found to contain as high as 80% rhenium. Since the UC used was very metal-rich (4.63% carbon), liquid uranium could be present in the carbide at the interface during the run and interacted with the rhenium clad to form the rhenium-rich phase observed by electron microprobe analysis.

Some of the interaction might have occurred during the bonding of the rhenium to the cast tungsten cup containing the UC wafer at 1900°C in the hot press. Unfortunately, no good bond could be formed by hot-pressing at lower temperatures (e.g., 1700°C) within a few hours. To avoid this difficulty, another rhenium-clad UC sample will be made for similar studies during the next quarter by sealing the interface between the rhenium and the tungsten cup containing the UC wafer by vapor-deposited tungsten. In addition to the rhenium-clad UC sample, two other diffusion-emission samples will be prepared for studies at 2073°K. These are W-25 Re-clad UC and vapor-deposited tungsten-clad UC. It is intended to use stoichiometric or slightly hyperstoichiometric UC in all these samples.

2.6. REFRACTORY-METALS INTERDIFFUSION

The purpose of this study is twofold: to gather information for the diffusion-bonding of refractory metals to tungsten, and to test the feasibility of duplex emitters in which a layer of better emitting materials, such as rhenium and iridium, is separated from the uranium-containing fuel by a layer of tungsten. The diffusion between tungsten and tantalum, and molybdenum and niobium, will be studied in the temperature range of 1200° to 2000°C, while the diffusion between tungsten and rhenium (vapor-

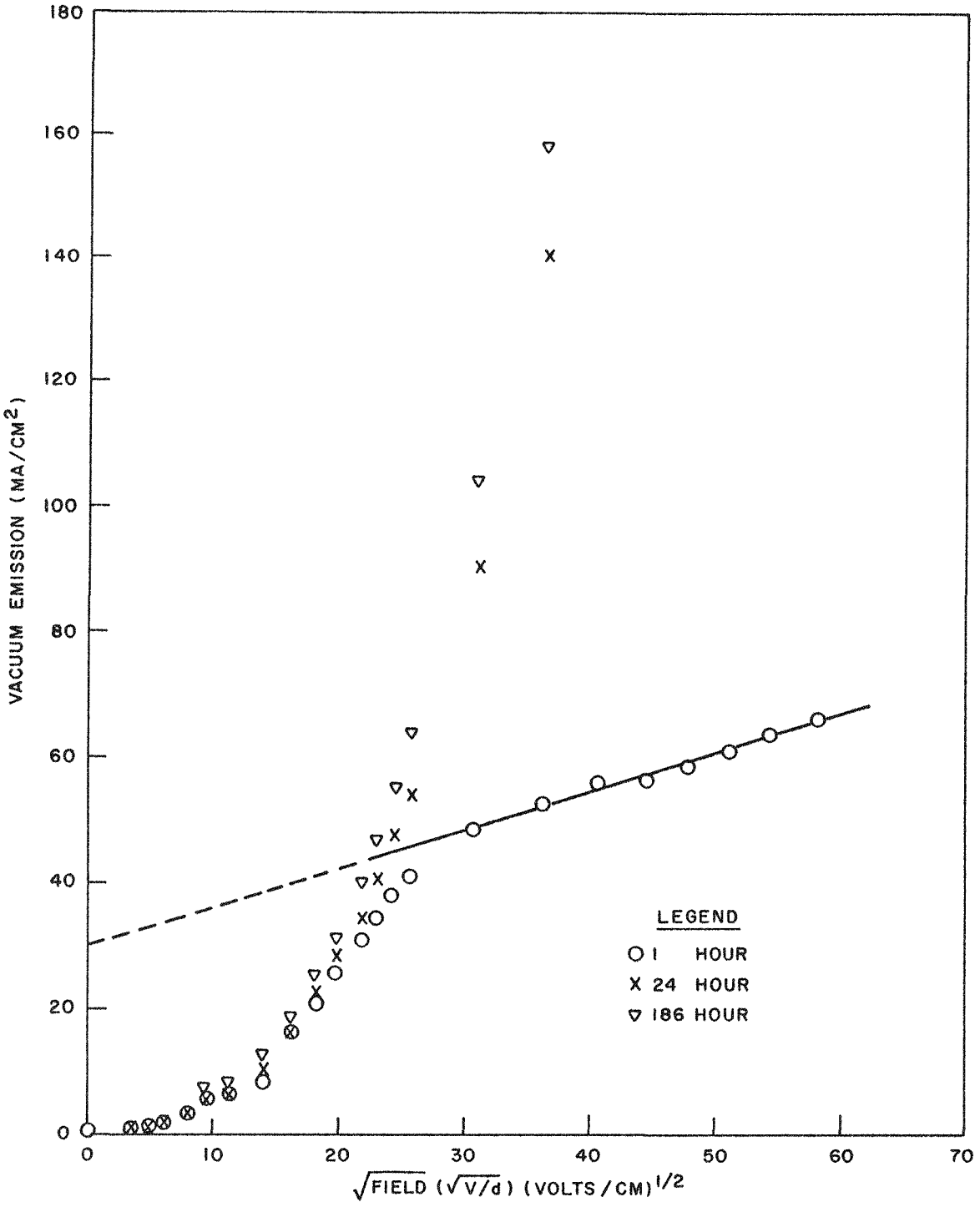

Fig. 2.8--Vacuum emission versus square root of field after sample E_1 (Re-clad UC) was maintained at 2063°K for various periods of time. Sample had been heated for 64 hr at 1923°K prior to obtaining data at 1 hr and 24 hr. After 170 hr at 2063°K, the sample was heated for 50 hr at 1663°K prior to obtaining data at 186 hr.

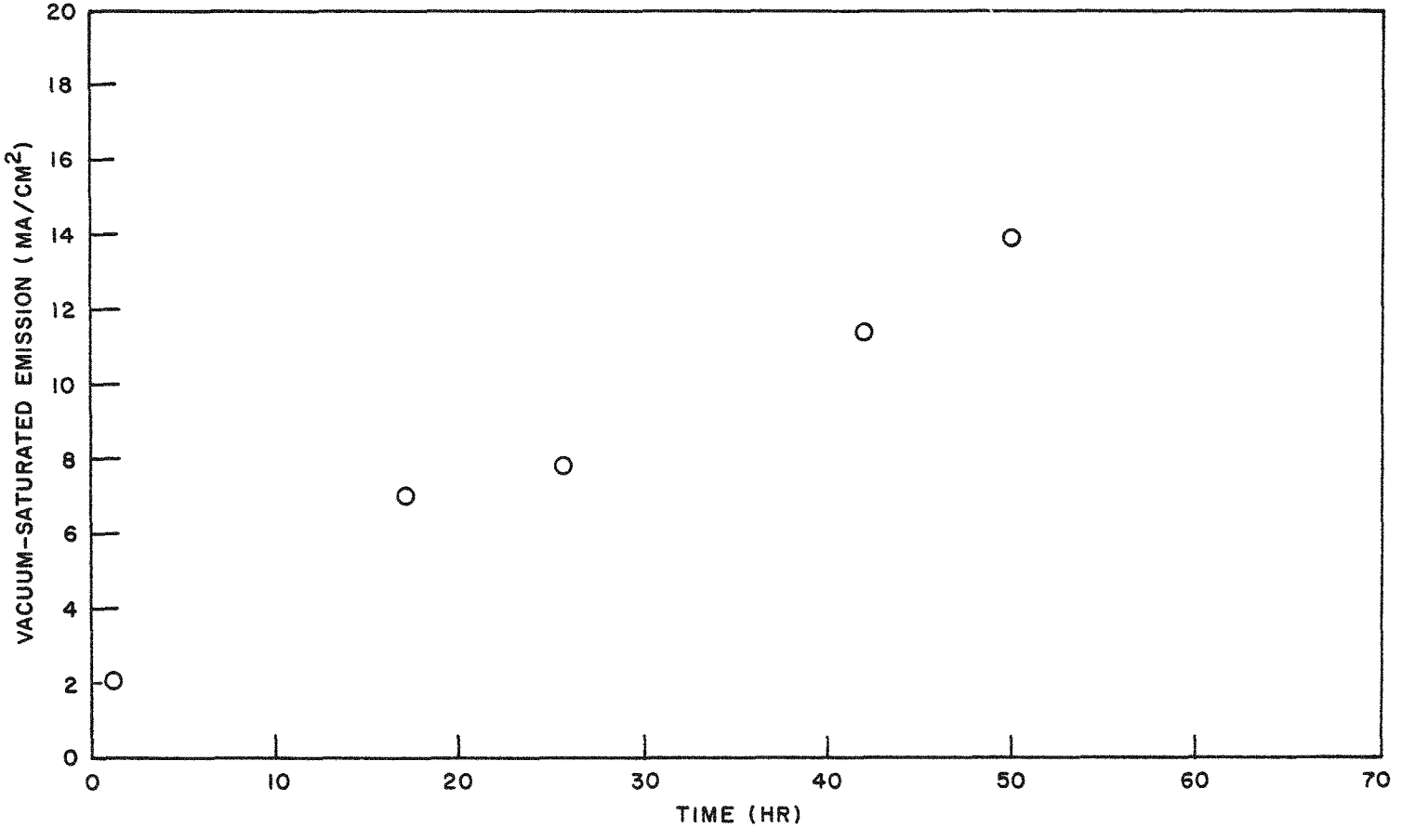

Fig. 2.9--Vacuum saturation emission versus time at 1663°K for sample E_1 (Re-clad UC) Sample had been heated at 1923°K and 2063°K for 64 hr and 170 hr, respectively, prior to obtaining data for this plot.

M-5745-1-2 (250×)

Fig. 2.10--Microstructures at the Re-UC interface of sample E_1

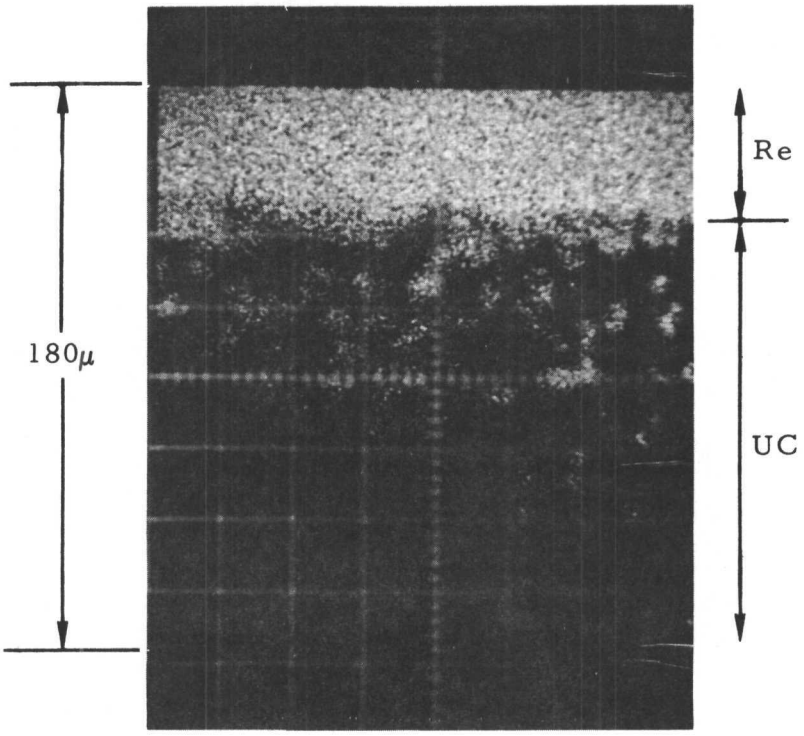

Fig. 2.11--CRT display of $Re_{M\alpha}$ near the Re-UC interface, showing rhenium penetration into the UC for a distance of about 100 microns

deposited) and iridium (vapor-deposited or electroplated) will be studied in the temperature range of 1400° to 2000°C.

The sequence of the experimental program is tabulated in Table 2.6. Duplicate runs will be made for each refractory-metal to tungsten combination at a given temperature. Initially, runs of 10-hr duration will be made to gain some preliminary information on the rates of interdiffusion of these systems. Runs of longer duration will be made if needed.

Table 2.6

REFRACTORY METAL-TUNGSTEN GROSS-DIFFUSION EXPERIMENTAL PROGRAM
(Numerical sequence of experiments to be performed)

Refractory Metal	Experimental Temperature (°C)				
	1200*	1400*	1600*	1800*	2000*
Iridium	(No test)	1	2	3	4
Rhenium	(No test)	1	2	3	4
Tantalum	5	1	2	3	4
Niobium	5	1	2	3	4
Molybdenum	5	1	2	3	4

*Duplicate runs will be made at each temperature.

The refractory metals required have been procured. These are electron-beam-melted tantalum and niobium, arc-cast tungsten and molybdenum, and chemically pure rhenium and iridium sheets. Experiments will be started early in the next quarter.

2.7. REFRACTORY-METALS DIFFUSION-EMISSION STUDIES

Rhenium and iridium layers over tungsten are to be studied. The purpose is to find out the feasibility of the concept of duplex-type emitters in which the tungsten provides a barrier between the carbide fuel and the emission-contributing materials such as rhenium and iridium.

During this period, one diffusion-emission cell of the design shown previously[2] has been fabricated and outgassed. The vapor-deposition of rhenium over vapor-deposited tungsten is being investigated. Chloroiridic acid needed for the electrodeposition of iridium over vapor-deposited tungsten has been obtained. It is expected that the preparation of samples should be completed during the next quarter, and the 1000-hr studies at 1800°C initiated.

2.8. MECHANICAL PROPERTIES OF UC-ZrC

During the last contract year,[1] measurements of the mechanical properties of UZrC fuels were initiated to derive strength and elasticity data for use in predicting the thermal-shock resistance and swelling behavior of fuels of various UC-to-ZrC ratios. During this effort, test equipment was developed and measurements were made on 10 UC – 90 ZrC, 80 UC – 20 ZrC, and UC in the temperature region 1600° to 1800°C. This year's program continues the previous efforts and will be extended to include a wider range of compositions, temperature, and strain rate, with controlled variations in porosity and microstructure.

The effort for this first quarter has been the modification to the test equipment. During the last contract year, the molybdenum support pedestal was found to have distorted because of severe side-loading. This occurred when the uranium carbide specimens being tested crept to a bow-shape before fracturing during testing at a low strain rate. The design of the sample support pedestal is currently being revised to develop more side-load resistance.

When the mechanical difficulties mentioned are corrected, measurements of modulus of rupture will proceed with UC, 50 UC – 70 ZrC, and 30 UC – 70 ZrC samples.

2.9. EMISSION-MICROSCOPY OF TUNGSTEN–URANIUM-CONTAINING CARBIDE CERMETS

It is believed that although uranium-containing carbides are excellent electron emitters in vacuum, their performance in cesium vapor is ion-generation-limited. The purpose of this study is to explore the possibility of improving their performance by incorporating high-work-function patches on the carbide surfaces. Uranium-containing carbide–tungsten cermets offer such a possibility. In order to achieve such a goal, however, the tungsten patches on the cermet surface would have to be able to maintain their high work-function in the presence of uranium-containing materials. Study of the electron emission patterns of these cermets at high temperatures as a function of time would indicate whether this will happen. The first samples selected for such studies are W-UC and W–(30 UC – 70 ZrC) cermets containing about 60 vol-% of carbides.

While these cermet samples were being prepared, a W-UO_2 cermet sample containing 60-vol-% UO_2 happened to be available. It was loaded into the emission microscope and studied at 1650°C for a period of 120 hr. Figure 2.12 is a photomicrograph of this sample, showing the dispersion of UO_2 in a tungsten matrix. An emission pattern taken after the sample was heated at 1650°C for 5 hr is shown in Fig. 2.13 (a). It can be seen

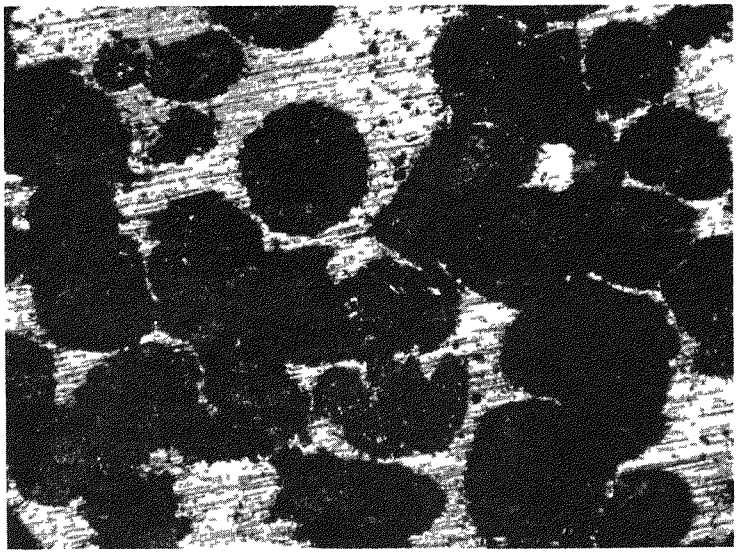

(100×)

Fig. 2.12--Photomicrograph of the U-UO_2 cermet sample studied in the emission microscope (60 vol-% UO_2)

that the UO_2 particles emit much better than the tungsten matrix, and a few cavities from which the UO_2 particles were lost by vaporization or by the polishing of the sample are clearly outlined by some fine UO_2 powder left. The surface thus is very heterogeneous in emission. Figures 2.13(b) and Fig. 2.13(c) are emission patterns taken from the same area of the sample after it had been at 1650°C for 50 hr and 120 hr, respectively. Although some of the UO_2 particles were lost by vaporization, the patchy nature of the surface remained. The study was terminated after 120 hr because the grid of the emission microscope became heavily coated with UO_2. Nevertheless, the results seem to indicate that higher-work-function areas may co-exist on a surface with the better-emitting UO_2. The W-UC and the W—(30 UC — 70 ZrC) cermets will be studied during the next quarter.

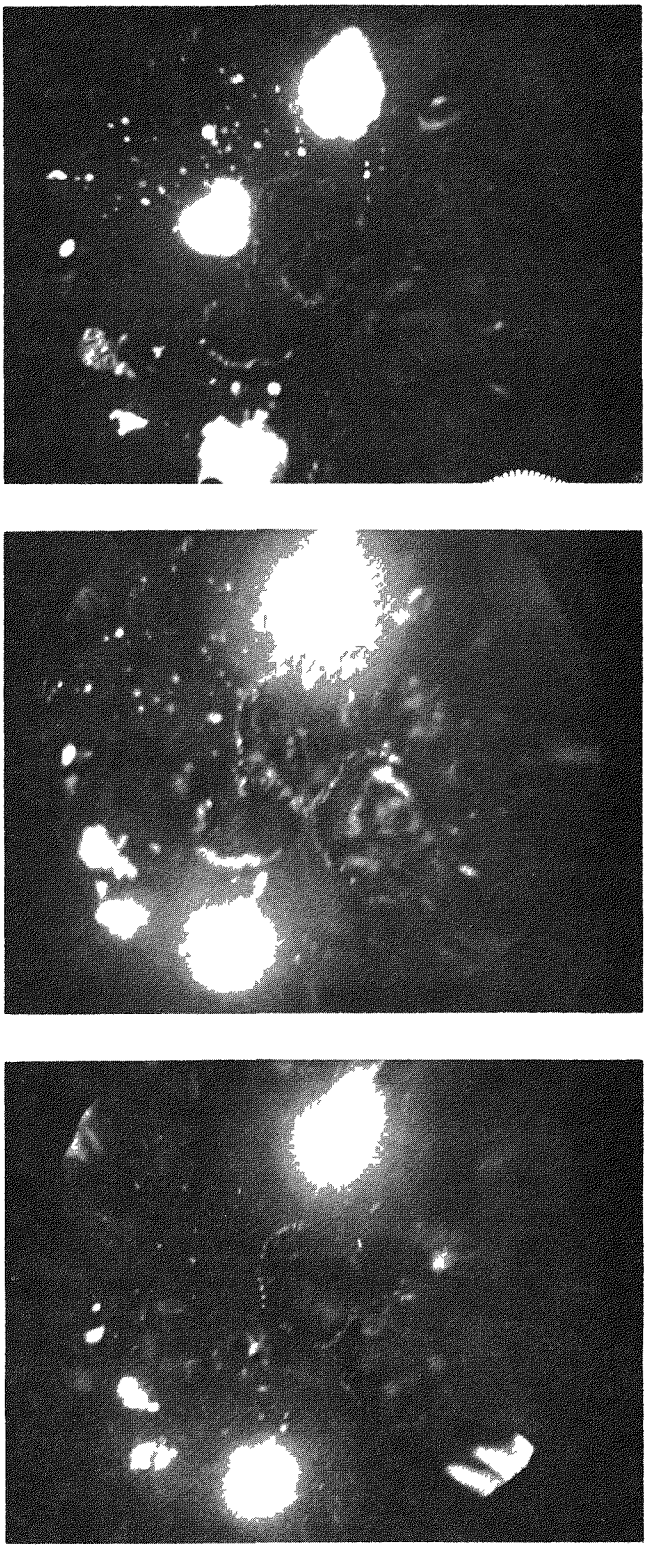

(a)
After 5 hr

(b)
After 50 hr

(c)
After 120 hr

Fig. 2.13--Emission patterns of a W-UO_2 cermet containing 60 vol-% UO_2 after heating at 1650°C for different periods of time; all three photographs are at ~90×

Section III

LIFE-TEST OF FUELED CESIUM CONVERTER

The program objective is to life-test fueled cesium thermionic converters up to 10,000 hr at a power density of 5 w/cm^2. From the test results with unclad UC-ZrC emitters, tungsten-clad UC-ZrC emitters, and semiclad cermet emitters, the long-term effects of evaporation and emission stability are to be investigated.

Toward this goal, the Materials-Life-Performance (MLP) converters were built and operated during the previous contract year[1] to meet a 1000-hr at 5 amp/cm^2 operational objective. Converter failures which were due to leaks in the tantalum emitter lead that forms part of the converter envelope and external corrosion from operating MLP converters in air detracted from the reliability of a long-term test.

A study was performed during this report period to determine the best method of fulfilling the experimental objectives. This led initially to a modification of a Mark I converter design, which is similar in geometry to the MLP converter. Its principal features were an integral, fueled, vapor-deposited tungsten emitter, an unguarded collector, and an ultrahigh vacuum environment for the converter envelope. It was concluded from this study that fabrication of a Mark I converter involved development of a new emitter structure, a new converter envelope, and new fabrication equipment for remote converter assembly.

During the Mark I design period, significant advances were made in the development of cylindrical geometry converters (Mark VI series) that employ vapor-deposited tungsten emitters. Four converters, including two in-pile cells, were tested without a termination due to converter performance failure. The fabrication technique for these converters is an established process with high standards in quality control.

These developments led to a parallel design study of the modifications required to adapt the Mark VI converter to the objectives of the Life-Test Program. If this is possible, an additional benefit is realized, that of testing a converter which relates to a cylindrical fuel-element design. The results of the study show that the cylindrical Mark VI series converter can fulfill the test objectives equally as well as the planar designs, and this design has an additional advantage in that the converter envelope and fabrication equipment are completely developed. It has been shown that the

development of the emitter structure involves about the same effort and time. In addition, the Mark VI test vehicle has a proven reliability up to 1,370 operating hours.

For these reasons, the design and fabrication development of a cylindrical fueled emitter has been initiated. It is intended for use in the first converter test scheduled for operation in February, 1964. Descriptions of both the plane and cylindrical converter designs, fabrication development, and test instrumentation are discussed in the following sections.

3.1. CONVERTER DESIGN

3.1.1. Mark I-G Planar-Geometry Converter

The Mark I-G converter, shown in Fig. 3.1, is mainly a redesign of the MLP converter to meet the program objective of operating up to 10,000 hr. The principal changes include:

a. Use of an integral, fueled, vapor-deposited tungsten emitter.

b. Elimination of the collector guard ring.

c. Operation in a high-vacuum environment.

A description of the complete Mark I-G design is given in the following sections.

Emitter Assembly (Mark I-G)

Two features of the MLP emitter assembly design that caused difficulty were (1) the thermal distribution due to electron bombardment and (2) failure of the cell due to leaks through the tantalum emitter support and filament housing. It was suspected that the two were related, i.e., local high temperatures in the tantalum were caused by nonuniform heat input from the filament. Also, the embrittlement of the tantalum may have been caused by contamination from the oil diffusion vacuum pump used for evacuation of the filament housing.

The emitter assembly is shown in Fig. 3.2. The clad-fuel emitter assembly is a planar geometry design similar to that of the MLP cell. It is fabricated by vapor-deposition coating of tungsten over UC-ZrC fuel pellets, which are inserted in a cup on the end of a preformed tungsten cylinder. A thermal analysis was made of the emitter structure using the RAT (Radial Axial Thermal) computer code. The analysis showed that a cylindrical helically wound filament resulted in a more uniform temperature distribution, as compared with a pancake filament which heats the end planar

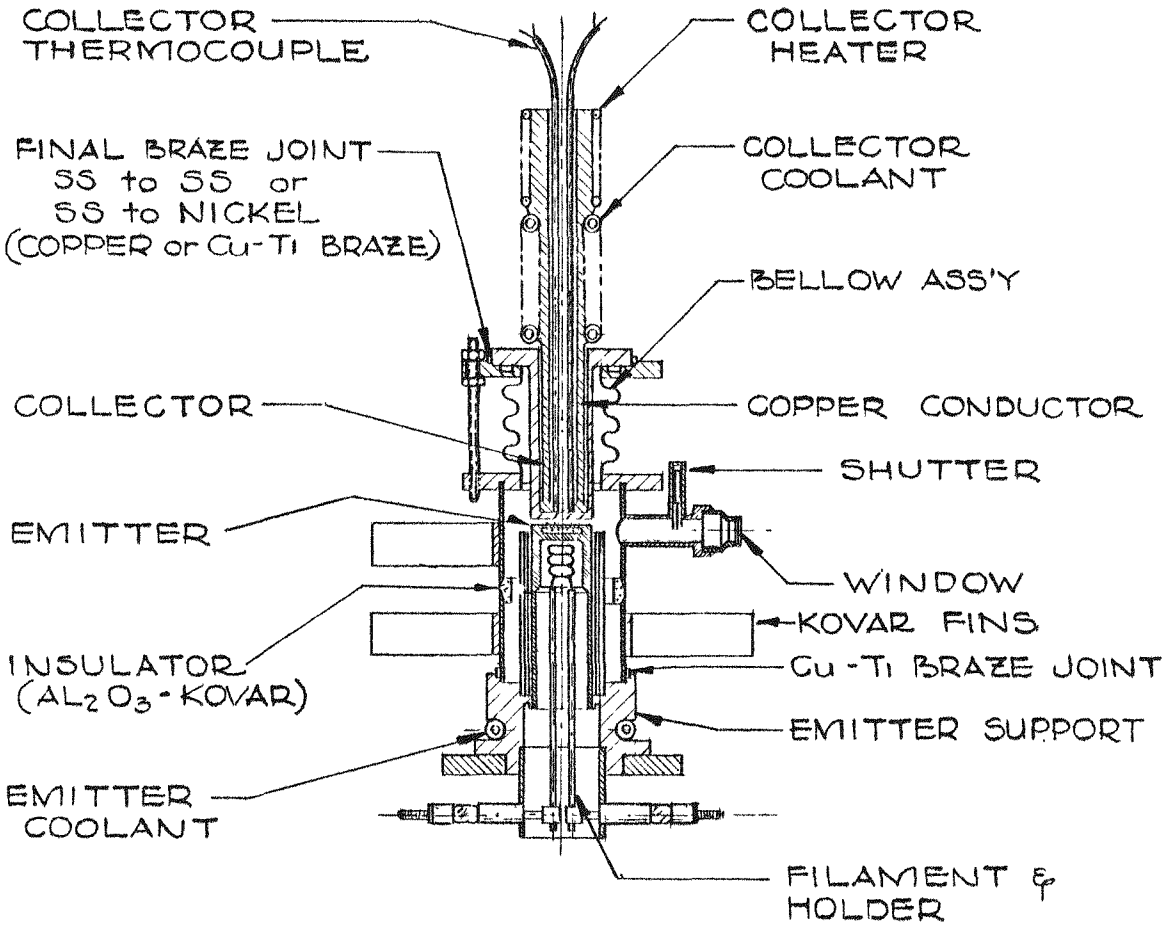

Fig. 3.1--Mark I cell design

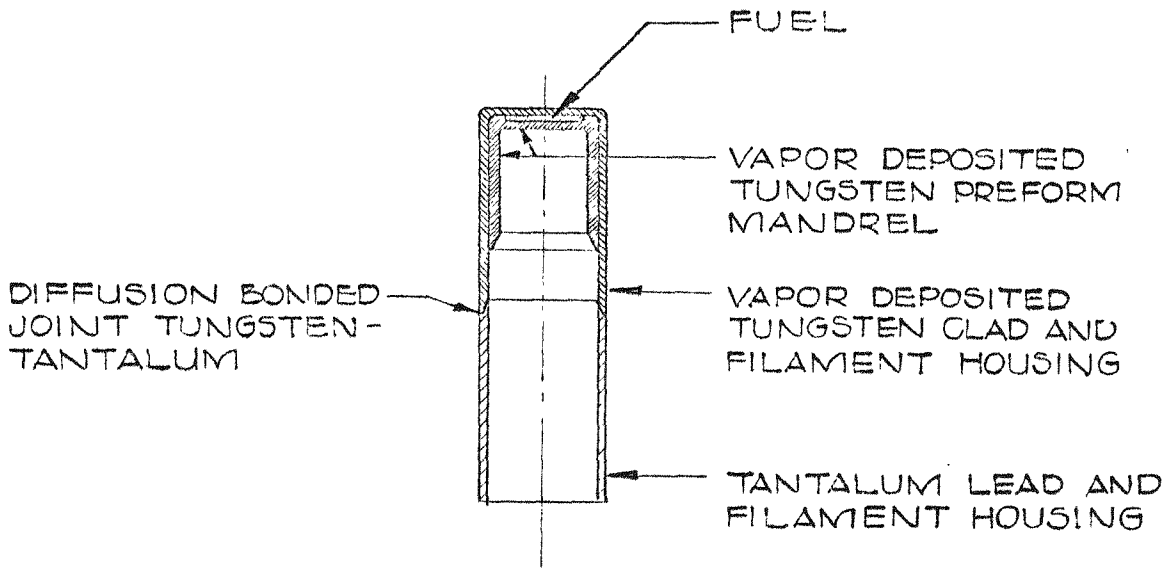

Fig. 3.2--Mark I emitter design

area only. The more uniform temperature distribution is due to the thermal resistance of the gap between the fuel and tungsten on the side facing the filament. The tungsten support is thick-walled (0.100 in.) opposite the filament and this thickness is then reduced to 0.050 in. at a distance of 1/2 in. below the filament where the tungsten is joined by diffusion-bonding to a tantalum stem lead. The tantalum stem is then joined by welding to a larger tantalum cylindrical block, which is a support for the interelectrode insulator. A gas cooling line is brazed to this block to remove about 200 watts of heat that is transferred by conduction and radiation from the emitter structure.

The emitter filament in the redesign operates in a vacuum environment pumped by an oil-free Vac-Ion pump. This should help to eliminate the embrittlement problem of the tantalum emitter support evidenced in the MLP cell design.

The design features that require development for this emitter assembly are the cladding of tungsten over the fuel and mandrel, and the subsequent diffusion-bonding of the tantalum support. Then, sufficient thermal cycling will be needed to prove the integrity of the bonds for 10,000-hr operation.

Collector Assembly (Mark I-G)

The cell was redesigned to operate without a collector guard ring; this redesign eliminated four additional braze joints, including a ceramic-metal insulator-seal, and generally simplified the fabrication. The cell was shortened to reduce the total thermal expansion and alignment problems.

The material of the collector is stainless steel, although nickel could be substituted for better collector surface properties. It was predicted that the required 5 watts/cm^2 output could be obtained with stainless steel collectors. However, the use of nickel is feasible, since the final joint to stainless steel is a copper braze and the expansion characteristics are similar.

The collector is cooled by conduction heat transfer through a copper conductor to nitrogen gas circulated through a 3/16-in.-diam stainless steel or Hastelloy helical tubing brazed to the conductor surface. The collector temperature variation is between 600°C minimum and 900°C maximum.

The fabrication of the collector assembly is considered straightforward and is simplified by elimination of the guard ring. This collector assembly design was considered to be free of major development problems.

Insulator-Bellows Subassembly (Mark I-G)

This subassembly was developed for the MLP cell for operation in air. The stainless steel flange and the bellows were joined by arc-welding, and a copper braze joint was made between the stainless steel flange and the Kovar bushing of the insulator. There were three main design features in this assembly for the Mark I design (see Fig. 3.1), as follows:

a. A method is provided for remote operation of the shutters for the emitter viewing windows while operating in vacuum. Two windows 90° apart allow parallel alignment of the electrodes and optical measurement of emitter temperature. The design provides an electromagnet which lifts an iron shutter away from the window.

b. Cooling of the insulator in vacuum is accomplished by Kovar radiation fins brazed onto the Kovar metal bushing of the insulator-seal.

c. A copper braze joint between the Kovar insulator bushing and the tantalum emitter support block increases its reliability because of the close matching of thermal expansion coefficients.

All the above three design changes require development and procurement of new materials. The transition joints between Kovar and stainless steel, and Kovar and nickel are new in the redesign. The development might involve joint redesign to minimize differential thermal expansion stresses and to correct misalignment of parts during fabrication.

Complete Assembly (Mark I-G)

The fabrication of the thermionic cell involves the final assembly of two subassemblies: the emitter and the collector, and the cesium reservoir. Each subassembly has several metal-to-metal joints, and the emitter subassembly has a metal-to-ceramic joint in the insulator. During final assembly, it is imperative that the cell be maintained in a clean condition and that the final assembly brazing not adversely affect joints previously made. One of the major difficulties is that each assembly step requires close dimensional control that can be obtained only by jigging and fixturing each subassembly before brazing. These operations are often performed on the bench, and assemblies are then vacuum-outgassed before brazing. For cylindrical-geometry cells, methods have been developed to perform assembly and jigging operations after outgassing has been completed without breaking the vacuum. In this way, it is possible to reduce the gas content of the cell to a point where previously made brazes are not affected by the heating of adjacent joints. This technique is thoroughly described under

the fabrication section for the Mark VI-E cylindrical converter, and the equipment is shown in schematic in Fig. 3.9, in Sec. 3.2.2. To accomplish this requires development of remote assembly and heating techniques in a high-vacuum brazing station. However, the station that is developed for the cylindrical-geometry converter is not suitable for the Mark I-G planar-geometry converter. A conceptual design of a high-vacuum remote assembly and brazing station is shown in Fig. 3.3. A description of the final-assembly procedure for this concept is given in Sec. 3.2.1.

Basically, the assembly brazing station shown in Fig. 3.3 is a high-vacuum operational test station. The converter must be heated and cooled in the critical areas with temperatures controlled in a manner similar to test operation. The design is even more complex because of the requirements for remote manipulation and alignment of components and heating sources for outgassing and brazing. The additional seals increase the vacuum pumping system requirements to attain the high vacuum desired for outgassing (10^{-6} to 10^{-7} torr at temperature).

3.1.2. Mark VI-E Cylindrical Converter

The Mark VI-E converter design is shown in Fig. 3.4. It features an all-refractory-material converter with a tungsten-clad fueled emitter, a molybdenum collector, a 0.010-in. interelectrode spacing, and vacuum environment operation. Emitter heating is by electron bombardment of its inner cavity. The thermal design permits independent variation of the operating parameters through two separate heating systems for the collector and cesium reservoir.

Emitter Assembly (Mark VI-E)

The emitter assembly, shown in Fig. 3.5, consists of (1) a vapor-deposited tungsten mandrel, (2) six fuel inserts, (3) a vapor-deposited tungsten cladding, and (4) a tantalum emitter stem. The emitter dimensions are 0.625 in. OD by 1.126 in. long, with a resulting area of 14 cm^2 as defined by the collector projection. Fuel inserts in the form of rectangular prisms, 0.15 in. wide, 1.126 in. long, and 0.06 in. thick cover 53% of the emitter area. The mandrel is preformed from a vapor-deposited tungsten cylinder and is then machined with slots for the fuel inserts. With the inserts precoated with tungsten and fitted to the slots, the entire mandrel is coated with tungsten by vapor-deposition. The emitter is finally ground to a finish size of 0.625 in. to give a clad thickness on the fuel of 0.042 in. This clad thickness is derived from thermionic-reactor design consideration.

The clad-fuel emitter is supported in cantilever by a hollow tantalum stem, which also conducts the current output to the emitter. The length-to-area ratio was chosen for optimum operation at an efficiency of 10% and

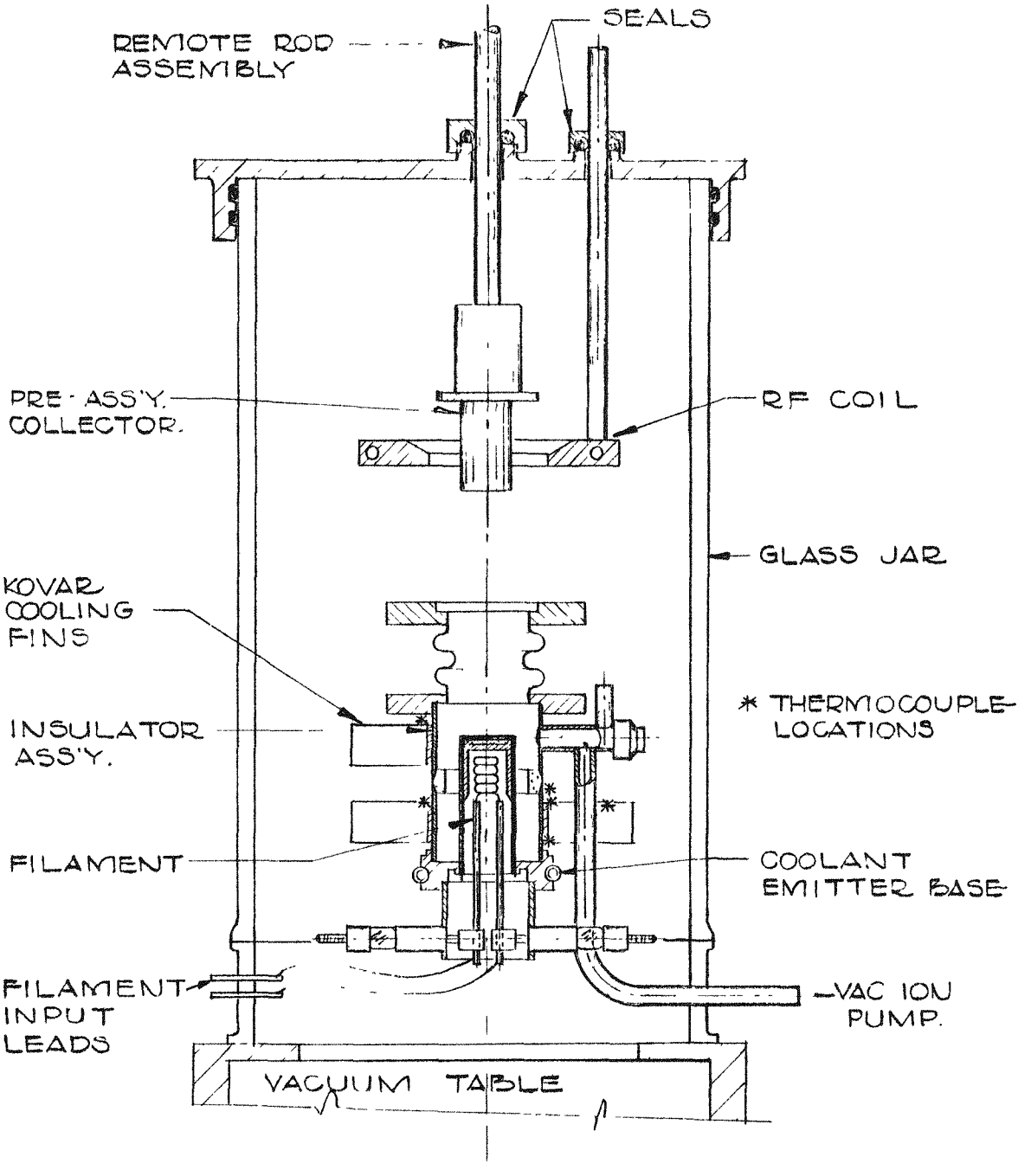

Fig. 3.3--Mark I remote cell assembly and brazing station

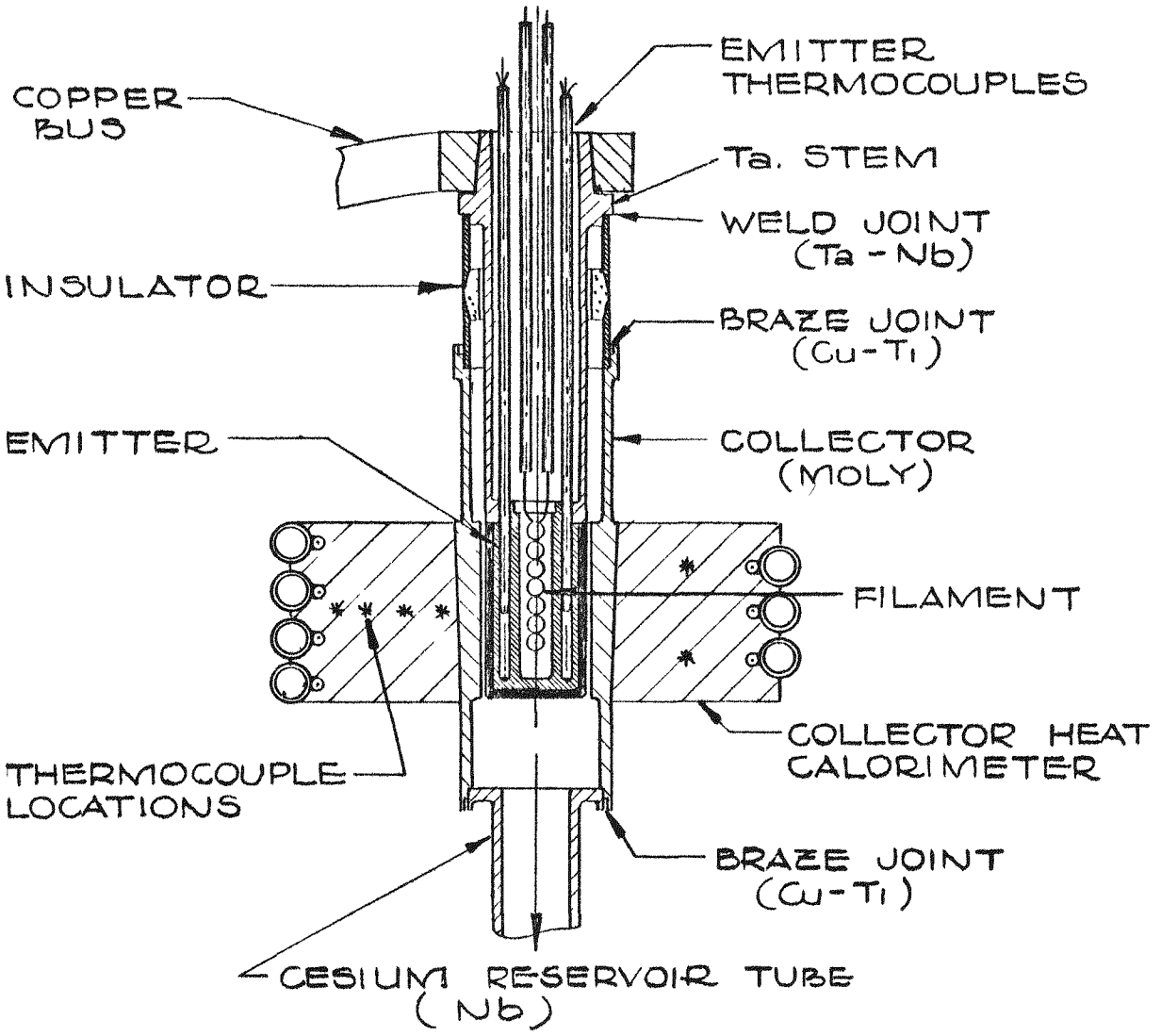

Fig. 3.4--Design of NASA life-test cell Mark VI-E

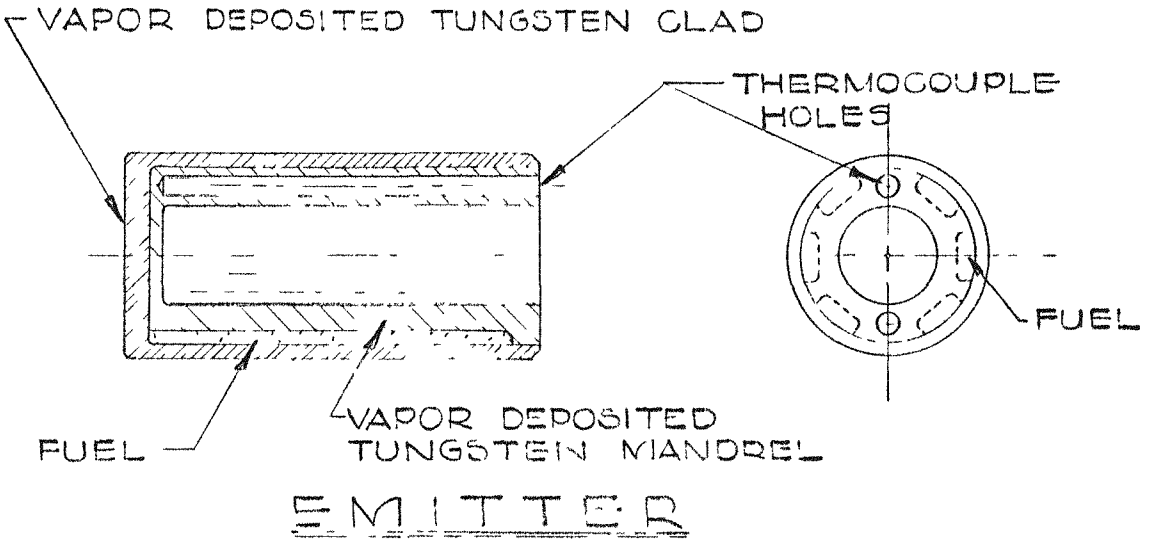

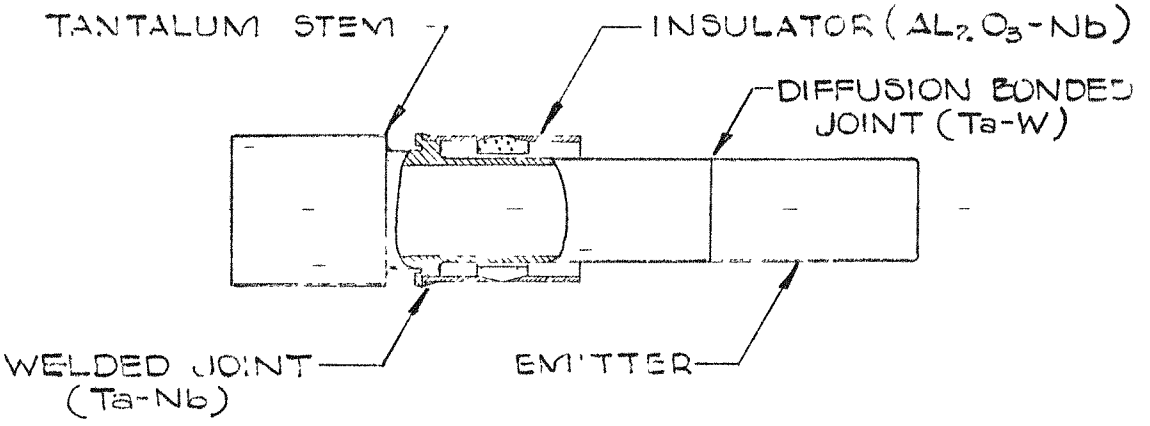

Fig. 3.5--Emitter and stem assembly of cell Mark VI-E

an output current of 10 amp/cm^2. The emitter stem dimensions are 0.625 in. OD by 0.565 ID by 1.89 in. long.

A ductile refractory metal was selected for the emitter stem, which maintains the emitter-collector interelectrode spacing. Since a cantilever design was chosen, there is a possibility of nonuniform expansion and resulting shorting of electrodes if care is not taken in choosing the stem material. Tantalum was chosen rather than niobium because its thermal expansion coefficient is closer to that of tungsten. Also, tantalum is easily diffusion-bonded to tungsten to form a tungsten-tantalum alloy at the interface. The cantilever support has maintained the emitter-to-collector spacing of 0.01 in. during 1300 hr of high-temperature operation. Post-test analyses of cell components have indicated that no problems developed in the cantilever support during the test period.

Collector (Mark VI-E)

The desired range of operating temperatures for the collector is 600° to 900°C. The refractory metals are more suitable for the collector because of their high-temperature strength and their thermal-expansion coefficients, which are very close to those of most ceramic electrical-insulator materials, as compared with nonrefractory metals. Molybdenum is the collector material for the Mark VI-E, primarily for the reason of superior thermionic performance.

The outer diameter of the collector is tapered and lapped to fit into a mating conductor heat-sink block as shown in Fig. 3.4. The waste heat from the collector is transferred across the conductor block to nitrogen gas circulated in a helical stainless steel or Kovar coil that is brazed in grooves on the outside diameter of the conductor. Several radially spaced thermocouples are included for measurement of radial temperature gradients to allow a rough estimate of the waste heat conducted from the collector. Two thermocouples measure the collector temperature.

An auxiliary heat source for collector temperature control is provided by a sheathed insulated nichrome wire heater brazed on the outside of the collector conductor. An additional temperature control is provided by varying the flow rate of the nitrogen-gas coolant in the cooling coil. This heat-transfer system is capable of maintaining the collector temperature within a range of 500° to 900°C.

Interelectrode Insulator (Mark VI-E)

The ceramic-metal insulator used in the Mark VI test cell is high-purity, high-density Al_2O_3 joined to niobium metal. The metal-to-ceramic seal is designed to be stress-free as far as possible. The choice of niobium

with alumina insulation was predicated on the fact that both materials have nearly the same thermal expansion coefficients; hence, the thermal stress in the seal is at a minimum. Since the niobium expands slightly less than Al_2O_3, the interface is in compression. At 800°C, the tensile stress in the niobium is 2000 psi, which is a factor of about 4 below its yield strength of 9000 psi.

The maximum creep of the niobium will be 0.0002 in., or about 0.02%, and the allowable creep-to-rupture is estimated to be about 1% for 10,000 hr operation at a tensile stress of 2000 psi and 800°C. The maximum operating temperature of the ceramic-metal seal is 850°C, and the normal operating temperature will be less than 650°C. The seal is made by copper brazing between the Al_2O_3 and niobium. These seals have operated continuously for over 1000 hr in a cesium environment of 10 mm Hg vapor pressure and temperature of 800°C or greater.

The heat sink for the emitter is by conduction along the copper bus to the environment. The thermal design assures that the insulator temperature is between 450° and 750°C, depending on the emitter temperature.

Interelectrode Spacing (Mark VI-E)

An interelectrode spacing of 10 mils is used for the Mark VI cell design. The primary engineering limitation on the spacing is determined by the close tolerance required between the insulator and the collector. This is because the final-assembly alignment between the emitter and the collector is obtained by self-jigging between the collector and the insulator on the emitter assembly. It has been demonstrated in the fabrication technique that this alignment method maintains a tolerance on the interelectrode spacing to within one mil, so that the spacing is maintained to within ±10%. The interelectrode spacing when the cell is at operating temperature is estimated to be 7 to 8 mils.

Cesium-Reservoir Assembly (Mark VI-E)

The cesium-reservoir tube (shown in Fig. 3.6) is made of niobium and is brazed to the bottom of the molybdenum collector. A copper tube welded to the cesium-reservoir tube is used for final bake-out, evacuation, and pinch-off sealing of the cell. Cesium is contained in a Kovar metal capsule within the niobium cesium-reservoir tube. The cesium vial is opened after final bake-out and pinch-off.

Two sheathed, insulated nichrome wire heaters are provided for cesium temperature control. The lower heater is used for maintaining the desired cesium temperature. It is automatically controlled and provides the bulk of the power for control. An auxiliary guard heater is wrapped

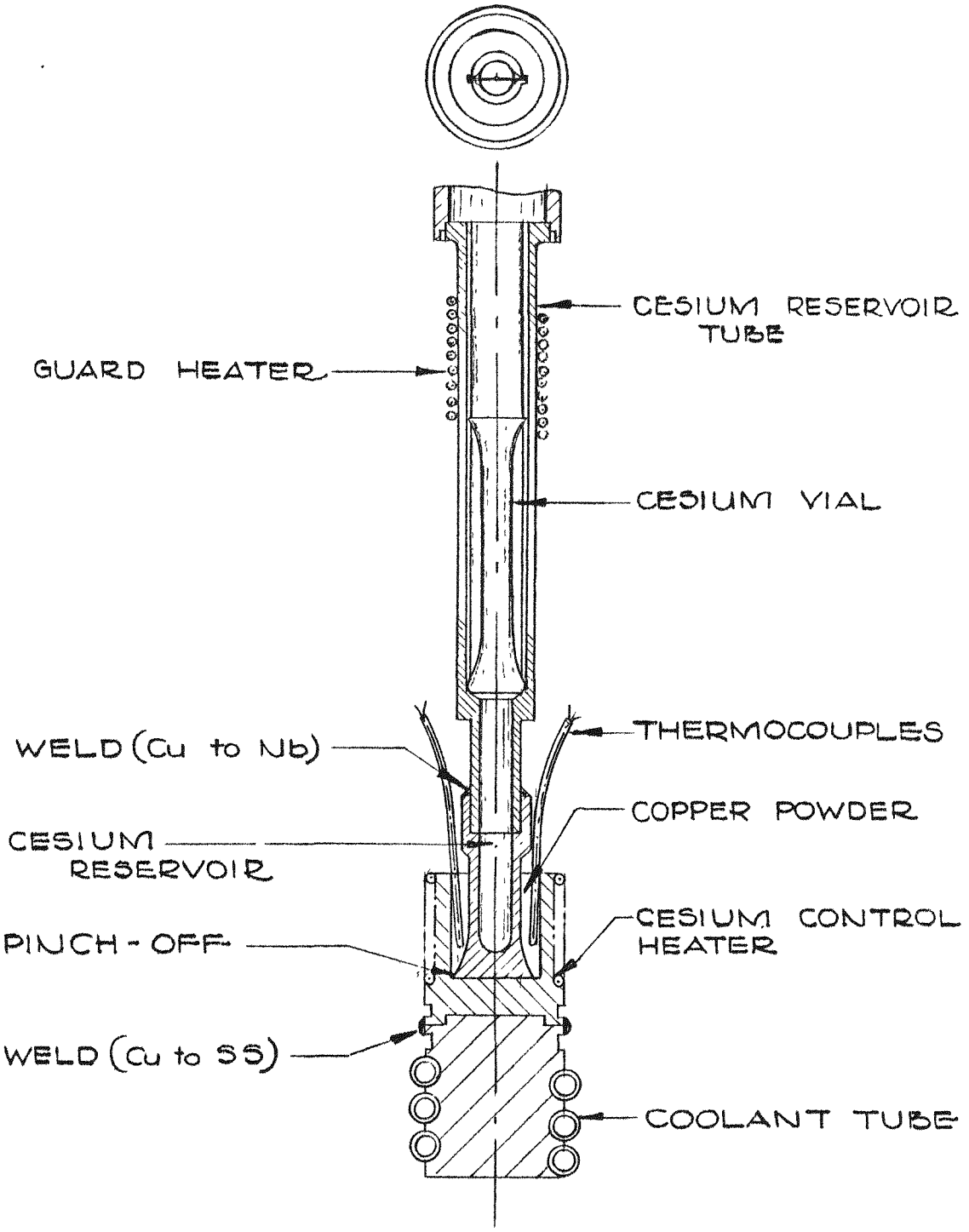

Fig. 3.6--Cesium reservoir of cell Mark VI-E

around the length of the cesium well. A tantalum radiation shield is wrapped over the guard heater. The heat for cesium temperature control is conducted to a stainless steel cylindrical block and then to nitrogen circulated through a stainless steel coil brazed onto the cylindrical block. The cesium temperature is automatically maintained by control of the current to the lower heater. The auxiliary heater current is manually adjusted to maintain the upper reservoir temperature at near collector temperature when the lower heater is controlling the cesium temperature.

3.2. CONVERTER FABRICATION

3.2.1. Mark I-G Planar-Geometry Converter

Upon completion of the Mark I-G converter design, a PERT scheduling was performed to show the long-lead items in cell development and material procurement. The results forecast a prototype-cell completion date on March 31, 1964.

The areas requiring fabrication development are: (1) the vapor-deposited tungsten-clad fueled emitter, and (2) the fabrication facilities and joining techniques to enable remote outgassing and assembly of the Mark I converter.

These development topics are discussed in detail below.

Fueled Emitter (Mark I-G)

Of five vapor-deposited tungsten blanks (one of which is shown in Fig. 3.7) from San Fernando Laboratories, Pacoima, California, two were specified for clad emitter structures and three for unclad emitters. All were chemically cleaned and outgassed at 1800°C to remove residual hydrogen from the thermochemical plating process. One emitter was machined into a base to accept one of six 30 UC – 70 ZrC fuel wafers which had been seal-coated with vapor-deposited tungsten. After final cleaning of the emitter and outgassing of the seal-coated 30 UC – 70 ZrC wafer, final cladding of the emitter base and fuel pellet into the fueled tungsten emitter form was performed by San Fernando Laboratories. The resulting fueled emitter, shown in Fig. 3.8, was outgassed to 1800°C.

Processing of this emitter into the final configuration involves preparatory machining and diffusion-bonding of the fueled tungsten emitter form to a tantalum stem by axial loading of the joint at a temperature of ~1800°C. This requires a direct loading on the fueled area, which is an undeveloped technique.

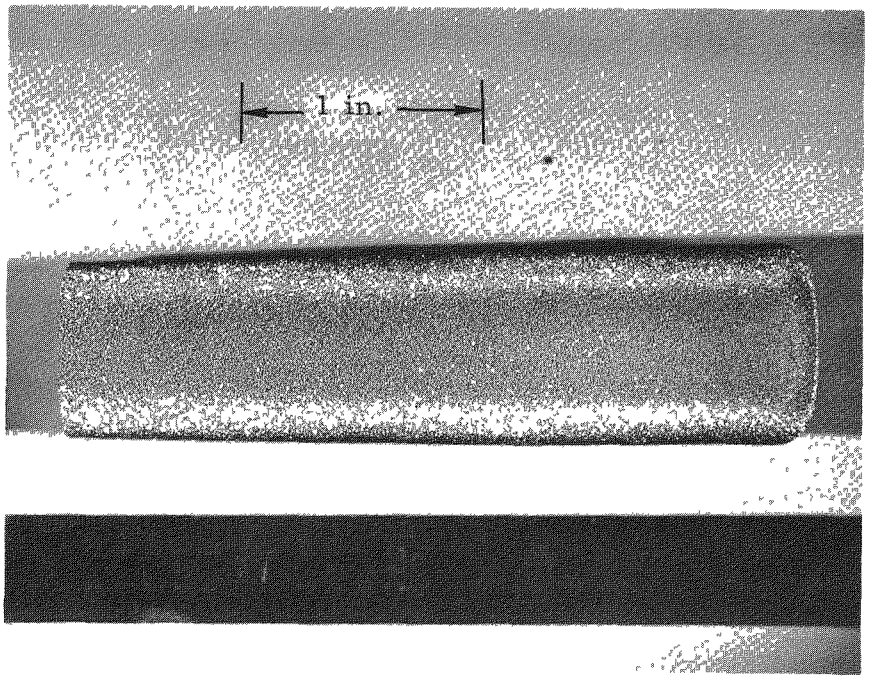

M-6395-2

Fig. 3.7--Vapor-deposited tungsten emitter blank for Mark I converter

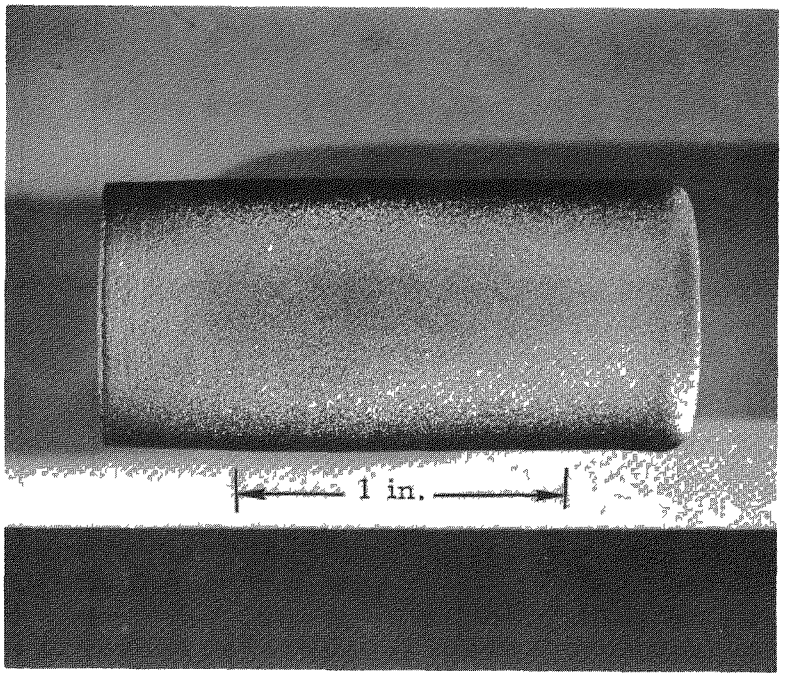

M-6395-1

(a) Side view

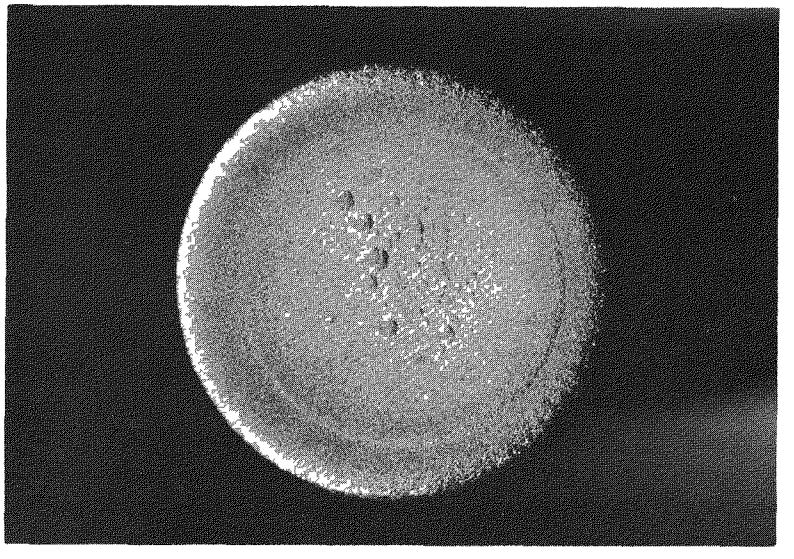

M-6395-3 (~3×)

(b) View of emitting surface; note pellet outline reproduced in the cladding layer

Fig. 3.8--Mark I emitter with 30 UC – 70 ZrC fuel wafer clad into the emitting surface before final machining

Insulator—Cooling-Fin Joining (Mark I-G)

The cell design in Fig. 3.1 includes Kovar radiation cooling fins attached to the Kovar insulator skirts. It is proposed to weld these fins to a support ring that is brazed to the Kovar skirts. The Kovar material required to initiate the fin-insulator fabrication is a long-lead procurement item. Therefore, the development of the technique for joining the insulator to the cooling fins could not be started until January, 1964.

Emitter Subassembly to Insulator Subassembly Joining (Mark I-G)

It is proposed to join the Kovar insulator skirt to the tantalum emitter support with a copper braze, using electron-bombardment heating of the emitter filament cavity. This type of brazing has been used for joining other materials with similar wetting characteristics and thermal expansion (tantalum to tantalum, niobium to tantalum, tantalum to molybdenum). Practice brazing is required to establish familarity with the joint configuration, braze wetting, and associated thermal gradients.

Development of Fabrication Facilities and Final Joining Techniques (Mark I-G)

Recent experience in the program for development of cylindrical-geometry converters established that ultraclean fabrication procedures were essential for acceptable performance. This guarantees that the initial power level is predictable, and that the evolution of residual gases does not cause converter degradation over long-term testing. It became obvious that fabrication techniques for the Mark I-G converter must also employ these same ultraclean procedures in that the design of the fabrication equipment and the fabrication sequence must allow for final outgassing and assembly of the cell to be accomplished remotely in vacuum. The development of this remote assembly equipment and of the necessary techniques is predicted to be one of the major development phases.

The conceptual design for the remote assembly apparatus shown in Fig. 3.3 provides that the collector subassembly be attached to the emitter, emitter-insulator, and bellows subassembly in a 2×10^{-7} torr vacuum environment. Both subassemblies are to be thoroughly outgassed in this high vacuum before the parts are joined and the final closure joint (bellows flange to collector) is brazed. The assembly procedure is detailed by the following steps:

1. Mount the subassemblies into the assembly stand. A Vac-Ion pump is attached to the cell final pinch-off tube, and critical joints are instrumented with thermocouples.

2. Outgas the collector to above the maximum operating temperature by induction heating in a vacuum of 1×10^{-6} to 2×10^{-6} torr.

3. Outgas the emitter and surrounding insulator components to above operating temperature (remaining below an unsafe fuel-clad temperature) by electron-bombardment heating of the emitter in a vacuum of 1×10^{-6} to 2×10^{-6} torr. Minimum cooling would be used in the emitter support block to limit the temperatures of the insulator joint, cooling-fin joint, and closed cesium ampoule to safe values.

4. Cool the components in vacuum ($\sim 2 \times 10^{-7}$ torr).

5. Position the collector in the bellows flange by moving the assembly rod through the vacuum seal.

6. Induction braze the collector subassembly to the bellows flange, and cool.

7. Leak-check the closure braze with the Vac-Ion leak detector.

8. With the cell exterior in vacuum, slowly heat the emitter to operating temperatures while pumping the cell internally with the Vac-Ion pump at 10^{-8} to 10^{-9} torr to further reduce the residual gas content of the cell.

9. Cool and leak-check the cell with the Vac-Ion leak detector.

10. Pinch off and weld the pinch-off.

The above outline illustrates that complex, reliable, and practicable assembly equipment must be designed and developed to effect the remote assembly of the Mark I cell. In addition, experimental studies would be necessary to select a brazing material and heating method required to assure reliability of the final braze joint.

3.2.2. Mark VI-E Cylindrical Converter

During the early Mark VI converter design-development cycle, the first few cells were assembled with the emitter closely spaced to the collector before final bake-out. Operation of these early refractory-metal cells revealed the characteristics of gassy or contaminated cells, e.g., the initial power level was low and further continuously degraded due to the build-up of contaminants on the collector surface. Outgassing of the cell interior after assembly required evacuation of contaminants through a 0.010-in. interelectrode space which has an extremely low conductance (0.055 liter/sec). Recognition of this problem resulted in the development of techniques to thoroughly outgas the emitter and collector prior to assembly, and subsequently to assemble the cell and effect the final braze seal without exposing the components to air. The assembly equipment and

joining techniques have been continuously improved during the past six months. The current status of the developed equipment and procedures is described in the following section.

Assembly Equipment and Procedures (Mark VI-E)

A sketch of the remote assembly and brazing station developed for the Mark VI cylindrical converter design is shown in Fig. 3.9. The station is essentially two vacuum systems: (1) A vacuum system built as an alignment fixture capable of pumping into the 10^{-7} torr range with a cold-trapped and baffled diffusion pump. This portion of the system aligns the emitter with the collector for assembly and has a quartz-glass assembly tube to allow heating of the emitter and collector subassemblies by an external induction field. (2) An ion-pumped vacuum system attached to the collector subassembly, capable of pumping into the 10^{-10} torr range.

The procedure to be used for assembly of the Mark VI-E life-test cell is described below:

1. The chemically cleaned, leak-tight, emitter-insulator and collector subassemblies are inserted into the assembly stand as shown in Fig. 3.9.
2. The emitter and collector are outgassed to above the expected operating temperature in a vacuum of 1×10^{-6} to 2×10^{6} torr by induction heating in separate steps.
3. The emitter and collector are cooled overnight in a vacuum of 1×10^{-7} to 2×10^{-7} torr and assembled (via the remote assembly rod) in vacuum. The insulator (which has been welded to the emitter stem) jigs and aligns the emitter to the collector.
4. The final braze is made by induction heating.
5. The assembly is cooled while continuing to pump the cell interior, and the final braze is leak-checked with the Vac-Ion leak detector.
6. The emitter is slowly heated by electron bombardment to 1500°C while the cell interior is being evacuated by the ion pump at a vacuum of 3×10^{-8} torr to further reduce the residual gas content of the cell. Fig. 3.10 illustrates this process with AEC cell OC-5.
7. After cooling, the cell pressure drops to 2×10^{-9} torr, and the cell is again leak-checked with the Vac-Ion leak detector.
8. The cell is pinched off and the pinch-off is welded.
9. The Kovar cesium ampoule is opened by mechanical deformation of the niobium cesium tube.

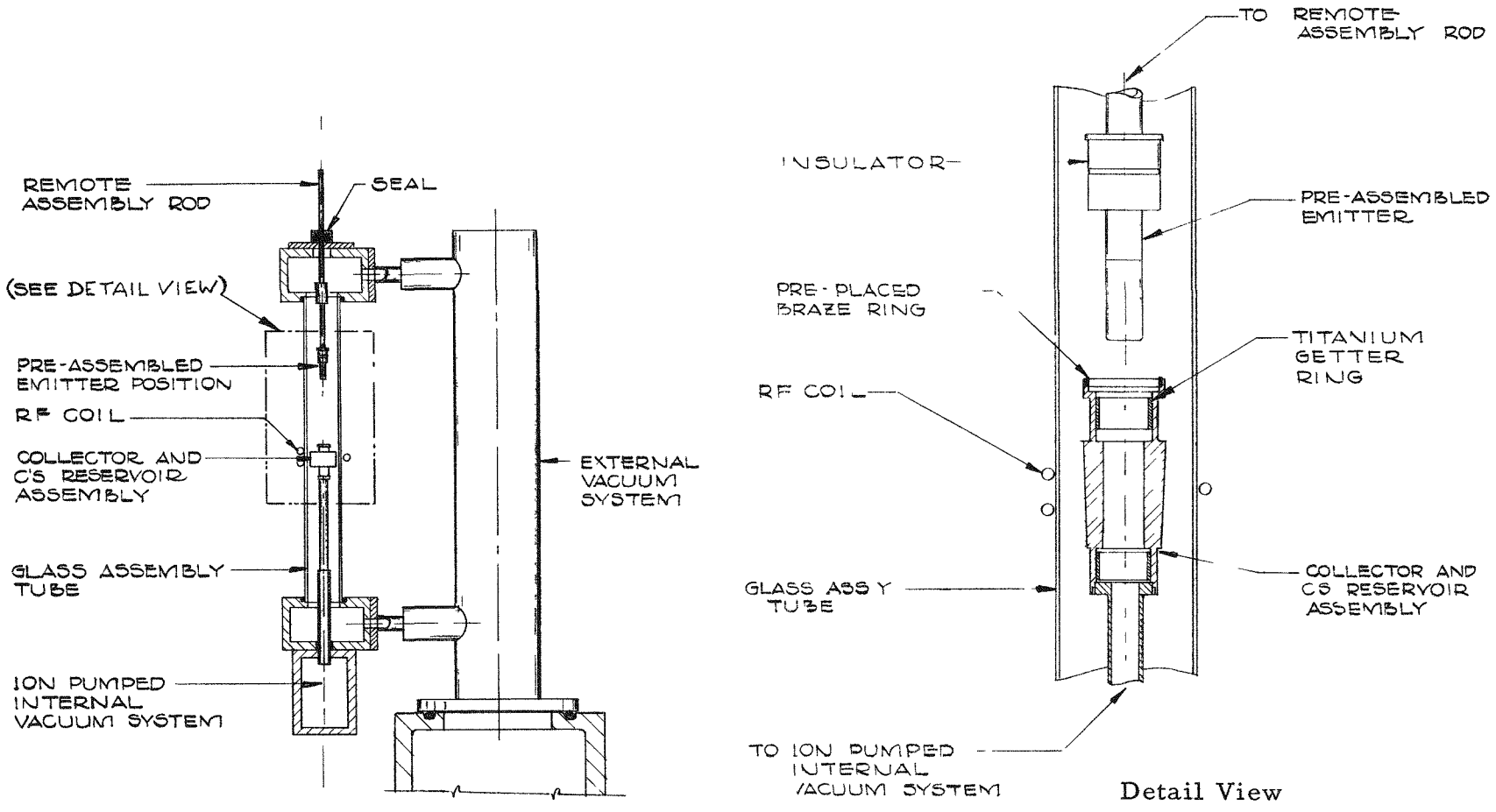

Fig. 3.9--Mark VI-E remote cell assembly and brazing station

TE-21993

Fig. 3.10--Apparatus for final assembly and bakeout of Mark VI converters

10. Gamma graphs are taken to establish the accuracy of the inter-electrode spacing.

Quality Control (Mark VI-E)

To augment the adopted methods of remote assembly for Mark VI cells, an exacting system of quality control and assurance has been instituted to control and inspect by metallography and chemical analysis incoming materials from vendors, and to apply rigid procedures for chemical cleaning, ultrasonic cleaning, and clean handling practices. In addition, welding and brazing practices have been upgraded by procedural control, joint design, and materials development to a point of 100% reliability.

Emitter Development (Mark VI-E)

Progress has been made toward development of a fueled prototype of the Mark VI emitter for a cylindrical-geometry life-test converter. Fabricating of the vapor-deposited emitter blank was initiated on November 1, 1963, at San Fernando Laboratories. The emitter blank was outgassed slowly to 1800°C and then machined, as shown in Fig. 3.11, to accept the 30 mol-% UC – 70 mol-% ZrC fuel forms. Subsequently, the emitter was outgassed to 1800°C with the fuel in place and was seal-coated, at San Fernando Laboratories. After outgassing the seal coat to 1800°C, the emitter was replated to above 0.585 in., was ground smooth to 0.585-in. OD to remove suspected structural imperfections (developed at fuel-fuel slot interfaces as a result of the plating process), and was final-plated to 0.654 OD. The appearance of the emitter as this stage is shown in Fig. 3.12.

The emitter was then slowly outgassed to 1800°C to remove hydrogen from the tungsten deposition process and machined for diffusion-bonding to a tantalum stem. The diffusion-bonding was accomplished in a vacuum chamber at 2×10^{-5} torr. The bonding pressure was 2200 psi at a joint temperature of 1800° to 1850°C. The fueled region of the emitter was held below 1850°C during diffusion-bonding to satisfy the tungsten–(90 UC – 10 ZrC) compatibility requirements.

Diffusion-bonding was successful in creating a leak-tight joint between the emitter and tantalum stem. The emitter stem assembly was machined to final form in preparation for thermal cycling to 1800°C to evaluate joint soundness.

The emitter development cycle will conclude with thermal cycling to 1800°C to determine if the diffusion bond can withstand the differential thermal stresses created and remain leak-tight. Before, during, and

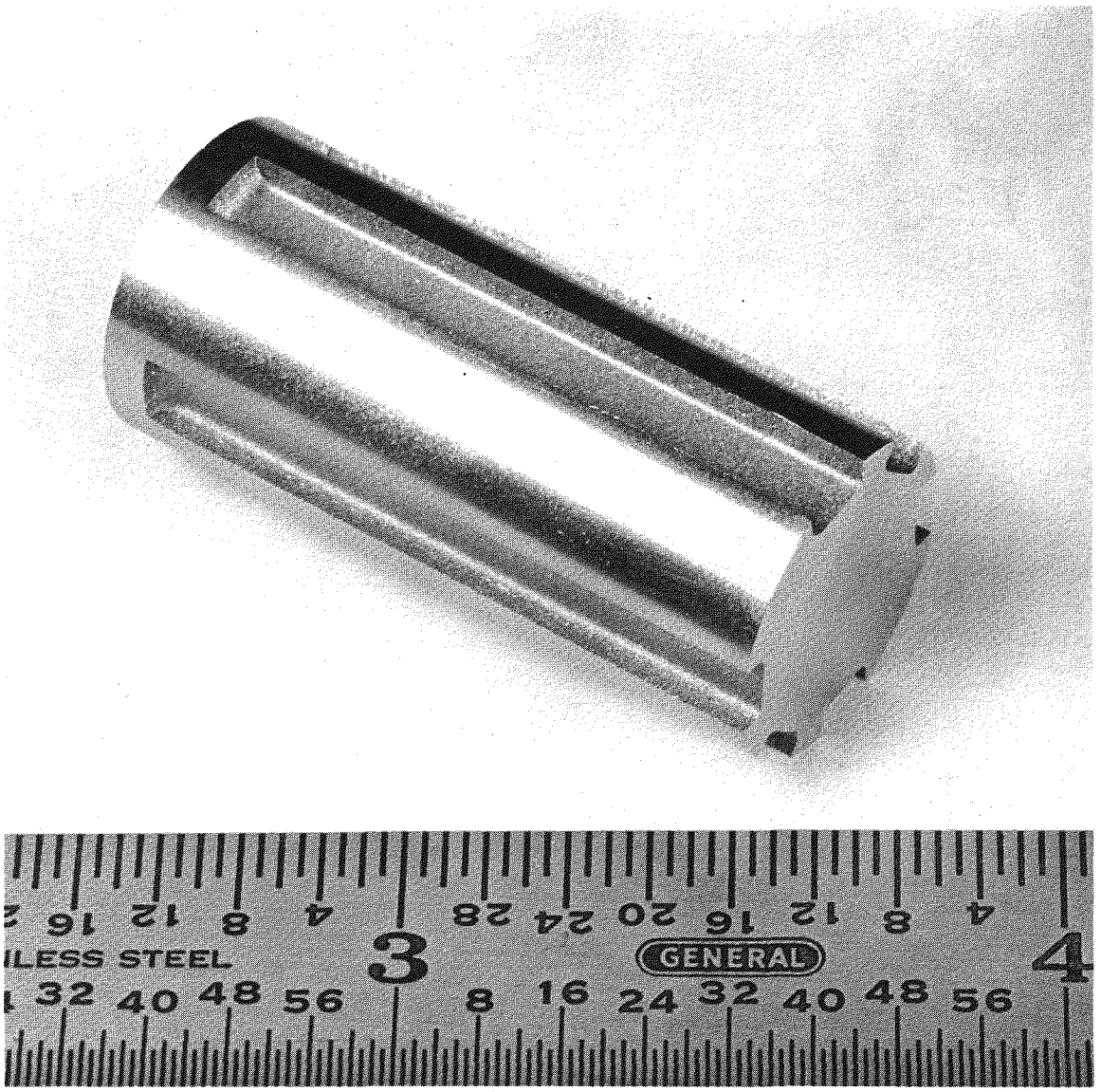

TE-24729

Fig. 3.11--Vapor-deposited tungsten emitter blank for Mark VI cylindrical-geometry cell, showing slots to receive 30 UC — 70 ZrC fuel slabs

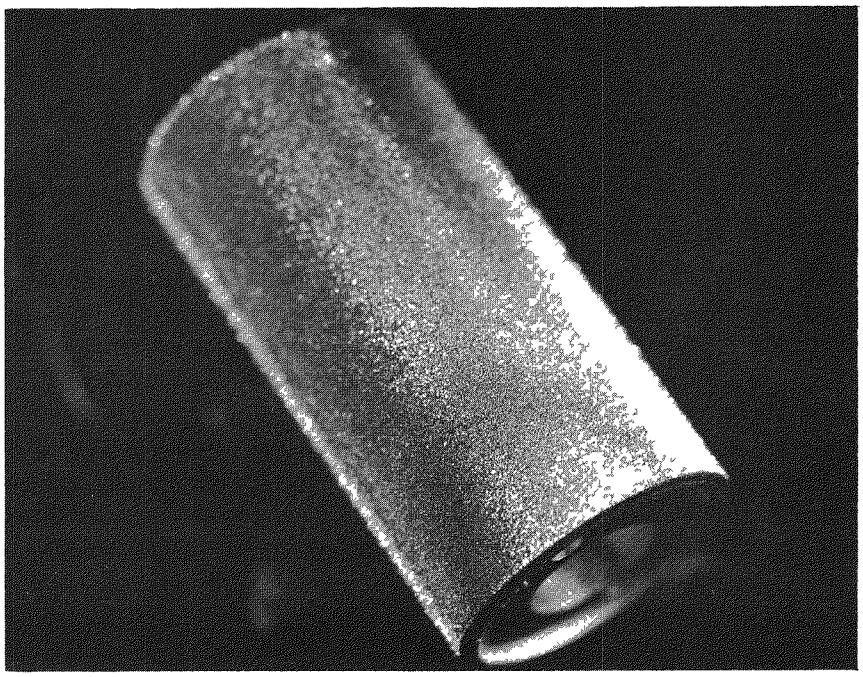

M-6063 (~2×)

Fig. 3.12--Vapor-deposited tungsten-(30 UC – 70 ZrC) emitter before grinding and diffusion-bonding to tantalum stem; note the two thermocouple wells

after thermal cycling, scintillation spectrometry will be used to establish that no fuel components are diffusing to the emitting surface. When the emitter development cycle is concluded, cell assembly will proceed, with completion of the first cell scheduled in February, 1964.

3.3. DESIGN SELECTION

A comparative study was conducted to determine the relative merits of the Mark I and Mark VI converter concepts as shown in Figs. 3.1 and 3.4, respectively. The study consisted of three phases: (a) comparison of the advantages of the Mark I and Mark VI designs, (b) comparison of the general design changes and development required for each concept, and (c) a detailed study of the planar and cylindrical emitter development. The results of the study are as follows:

1. Fabrication of the Mark I converter involves development of the collector-insulator envelope, whereas the envelope of the Mark VI is already developed and has reliably operated for more than 1300 hr.
2. The equipment for remote fabrication-assembly of the Mark I must be developed and fabricated. The procedures and equipment for remote fabrication-assembly of the Mark VI are available now.
3. The emitter development is estimated to be about equal for the two designs.
4. The Mark VI emitter design gives a fuel-to-tungsten area ratio of 53% as compared with 40% in the Mark I design.
5. The Mark VI converter produces power at 11 w/cm^2 at an emitter temperature of 1800°C and at a cold interelectrode spacing of 0.010 in. In addition, the energy characteristics and temperature profiles are well known for the Mark VI converter.

Modification of the Mark VI cylindrical-geometry thermionic converter design for the converter life-test program has definite fabrication advantages over use of the newly designed Mark I-G cell. The estimated completion date of the Mark VI life-test converter is January 31, 1964, versus March 31, 1964, for the Mark I cell. This disparity in completion dates arises from the difference in developmental input required for each cell. Fabrication of the Mark VI cell has been developed under an AEC contract to the point of reliable operation.

These considerations indicate that emphasis should be placed on the development of cylindrical cells. The experimental program has been planned accordingly.

3.4. CONVERTER TESTING

3.4.1. Test Equipment

An eight-test-station complex was designed for NASA converter life-testing. Figure 3.13 shows the vacuum stand mounted in a cabinet together with the heater supply, the pump power supply, and the converter load circuit. The second cabinet contains converter temperature controllers. To obtain filament life of 2000 to 3000 hr and to prevent oxidation of the cell envelope for 10,000 hr, ultrahigh-vacuum ion pumps capable of achieving 10^{-9} torr are employed. These pumps have the additional advantage of being fail-safe, i.e., an electrical power failure would not endanger the life-test. The vacuum system includes a 100 liter/sec ion pump with a 12-in. glass bell-jar and a Viton gasket. Nine ports with all-metal seals are provided for the admission of eight sheathed Chromel-Alumel thermocouples, four 1/4-in. stainless steel cooling lines, four heater circuits, two high-current conductors, and four compensated leads for the emitter thermocouples. The system is roughed with Vac-Sorb pumps to eliminate any possibility of contamination by forepump oils. Only one roughing system is provided, and it is mounted on a cart for mobility.

The emitter is heated by a helically wound tungsten filament and a regulated electron-bombardment supply. The regulation of the bombardment current provides a constant emitter temperature during unattended operation. The emitter temperature is monitored with two (replaceable) sheathed tungsten/tungsten—26% rhenium thermocouples. The sheath is 1/16-in.-diam tungsten—26% rhenium. One of the thermocouples is used for emitter temperature recording, the other in conjunction with a limiting device that will disconnect the bombardment voltage when a preset maximum temperature has been exceeded. It also actuates a warning light when a preset minimum emitter temperature is sensed, indicating a malfunction of the control circuit.

The collector and cesium reservoir temperatures are each measured by two Chromel-Alumel thermocouples, one for recording and the other for controlling. Collector temperature regulation is accomplished through a duration-type controller that actuates a cooling-air solenoid valve. The cesium-reservoir temperature is maintained by a time-proportioned temperature controller with a 1/2% accuracy. Both controllers are equipped with panel meters so that the cesium-well temperature may be visually monitored continuously.

A 200-channel electronic data logger measures converter temperatures as well as input and output power. These data are then processed through a reader and a computer with the resulting output printed in a tabulated form or plotted. The logger can be slowly stepped through each

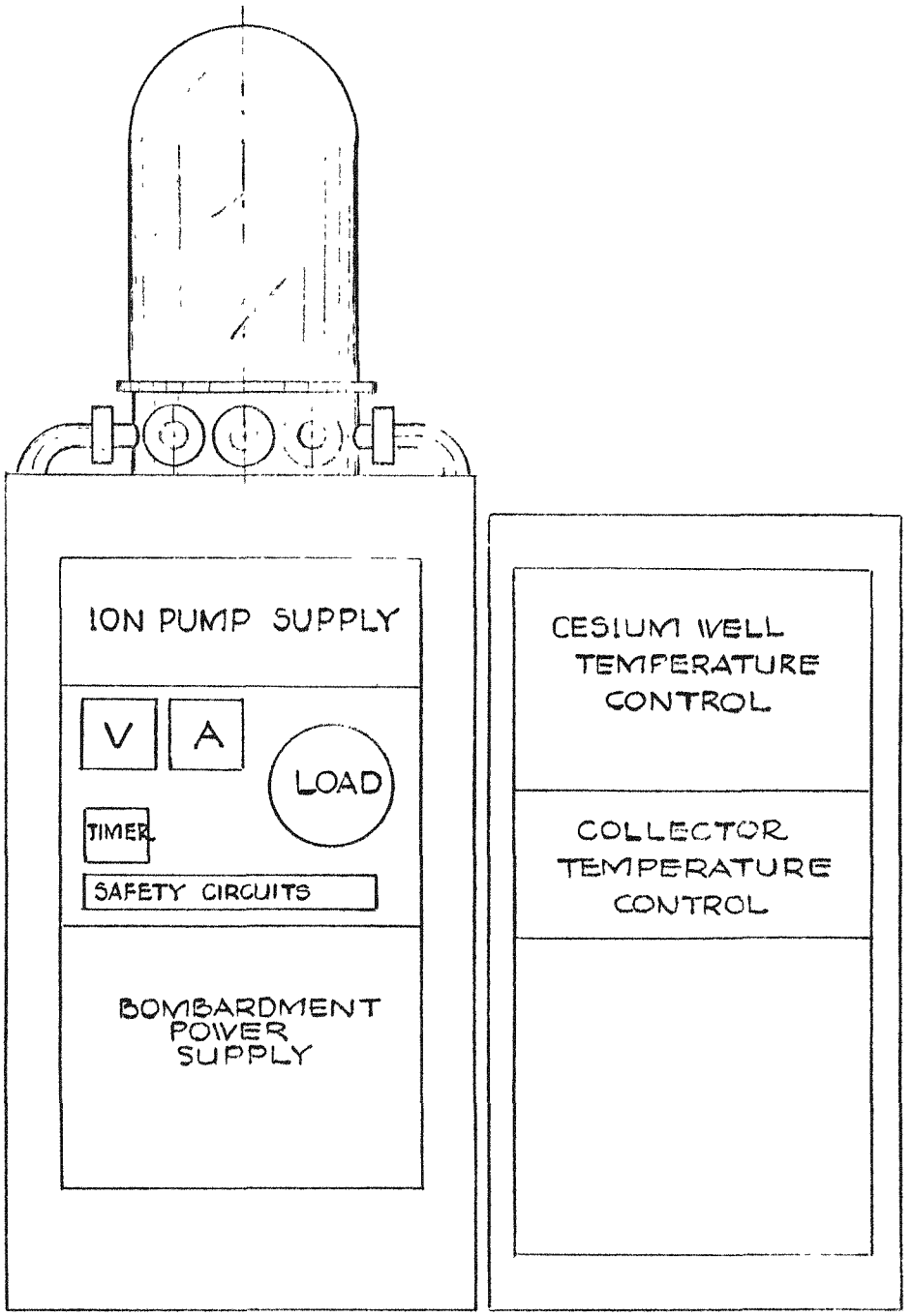

Fig. 3.13--Converter life-test station

channel enabling the operator to observe and manually record any desired data. In addition, provision is made to observe the input and output power on conventional voltage and current meters.

3.4.2. Operating Plan

The operating procedure includes a preliminary testing phase prior to the long-term uninterrupted steady-state test. In the preliminary operation, a limited amount of detailed performance analysis will be done to determine the optimum operating conditions, to establish reference points for later performance checks, and for comparison with the operating characteristics of previous converters. This type of data is essential in determining the degree of performance reproducibility among converters with identical geometries and materials, and in determining the long-term effects on thermionic performance.

Section IV

IRRADIATION STUDIES

Under the present contract, three capsules are to be irradiated in the NASA Plum Brook Reactor. The purpose of these irradiation experiments is to extend our understanding of irradiation behaviors (such as dimensional stability and fission-product-release properties) of candidate thermionic cathode materials to a period equivalent to 5000-hr operation of thermionic fuel elements. The materials to be studied will be selected on the basis of the results obtained under Contract NAS 3-2532.[1] These capsules are

1. Capsule containing unclad UC-ZrC specimens at 1800°C.
2. Capsule containing metal-clad uranium-bearing fuels at 1800°C.
3. Capsule containing metal-clad uranium-bearing fuels at 1500°C.

In view of the long lead-time needed for gathering the nuclear information and the preliminary designs of the capsule and its associated mechanical components so that a request to use the Plum Brook Reactor can be made to its Policy Committee, the following tasks were initiated on August 15, 1963, and continued to October 13, 1963, under an extension of Contract NAS 3-2532:

1. Calculation of the neutron flux distribution as a function of control-rod position in the V-tube of the Plum Brook Reactor, where it is planned to perform the irradiation experiments.
2. Calculations of the sample temperature based on the information obtained in 1, above, and the heat-transfer characteristics for the clad capsule design used under Contract NAS 3-2532.
3. Preliminary design of the capsule positioning and flux control mechanism.
4. Preliminary design of the cooling system.

The results obtained have been reported in the final report under Contract NAS 3-2532.[1] A manuscript incorporating such information was assembled in November, 1963, and submitted to the Policy Committee

of the Plum Brook Reactor as "Request For Irradiation for Plum Brook Reactor Facility Experiment 62-13R1." It is expected that a presentation will be made before the Policy Committee some time early in December, 1963, on the contents of this manuscript for the approval of the Committee on the use of the Plum Brook Reactor for the irradiation experiment.

REFERENCES

1. Yang, L., et al., "Investigations of Carbides as Cathodes for Thermionic Space Reactors, Final Report" (Contract NAS 3-2533), General Atomic Report GA-4769 (to be issued).

2. Weinberg, A. F., et al., "Investigations of Carbides as Cathodes for Thermionic Space Reactors, Final Report, May 15, 1961, through August 31, 1962" (Contract NAS 5-1253), General Atomic Report GA-3523.

3. Yang, L., et al., "Carbide Cathode Studies: Physical and Chemical Redeposition, Final Report" (Contract NAS 3-2301), General Atomic Report GA-3642, January 30, 1963.

4. Penrice, T. W., "Special Ceramics," Proceedings of Symposium, P. Popper, ed., British Ceramic Research Association, 1960.

5. Brunauer, S., P. H. Emmett, and E. Teller, J. Am. Chem. Soc., 60, 309 (1938).

DISTRIBUTION LIST

1. Advanced Research Projects Agency
   The Pentagon
   Washington 25, D. C.
   Attn: John Huth

2. Aerojet General Nucleonics
   San Ramon, California
   Attn: K. Johnson

3. Aerospace Corporation
   El Segundo, California
   Attn: Librarian

4. Air Force Cambridge Research Center
   (CRZAP)
   L. G. Hanscom Field
   Bedford, Massachusetts

5. Air Force Special Weapons Center
   Kirtland Air Force Base
   Albuquerque, New Mexico
   Attn: Maj. H. W. Baker
   Chief, Nuclear Power Division

6. Air Force Systems Command
   Aeronautical Systems Division
   Flight Accessories Laboratory
   Wright-Patterson AFB, Ohio
   Attn: ASRMFP-2/E, A. E. Wallis

7. Allison Division
   General Motors Corporation
   Indianapolis 6, Indiana
   Attn: T. F. Nagey

8. Aracon Laboratories
   Virginia Road
   Concord, Massachusetts
   Attn: S. Ruby

9. Argonne National Laboratory
   9700 South Cass Avenue
   Argonne, Illinois
   Attn: Aaron J. Ulrich

10. I. I. T. Research Institute
    10 West 35th Street
    Chicago, Illinois 60616
    Attn: D. W. Levinson

11. Astropower, Incorporated
    2121 Paularino Avenue
    Newport Beach, California
    Attn: Lou H. Mack

12. Atomics International
    P. O. Box 309
    Canoga Park, California
    Attn: Robert C. Allen
          Charles K. Smith

13. The Babcock & Wilcox Company
    1201 Kemper Street
    Lynchburg, Virginia
    Attn: Frank R. Ward

14. Battelle Memorial Institute
    505 King Avenue
    Columbus 1, Ohio
    Attn: David Dingee
          Don Keller

15. The Bendix Corporation
    Red Bank Division
    Northwestern Highway
    Detroit 35, Michigan
    Attn: M. L. Dring

16. Brookhaven National Laboratory
    Upton, Long Island, New York
    Attn: Dr. O. E. Dwyer

17. Bureau of Ships
    Department of the Navy
    Washington 25, D. C.
    Attn: B. B. Rosenbaum

18. United Aircraft
Pratt & Whitney Canel Facility
Middletown, Connecticut
Attn: M. DeCrescente

19. CANEL Project Office
USAEC
P. O. Box 1102
Middletown, Connecticut
Attn: H. Pennington

20. Consolidated Controls Corporation
Durant Avenue
Bethel, Connecticut
Attn: David Mende

21. Douglas Aircraft Company
Missile and Space Engineering
Nuclear Research (AZ-260)
3000 Ocean Park
Santa Monica, California
Attn: A. Del Grosso

22. Electro Optical Systems, Inc.
300 North Halstead Avenue
Pasadena, California
Attn: A. Jensen

23. Sperry Rand Corporation
Ford Instrument Division
32-36 47th Avenue
Long Island City, New York
Attn: T. Jarvis

24. General Electric Company
Missile & Space Vehicle Department
3198 Chestnut Street
Philadelphia 4, Pennsylvania
Attn: J. C. Danko

25. General Electric Company
Knolls Atomic Power Laboratory
Schnectady, New York
Attn: R. Ehrlich

26. General Electric Company
Power Tube Division
One River Road
Schnectady 5, New York
Attn: D. L. Schaefer

27. General Electric Company
Nuclear Materials & Propulsion Operation
P. O. Box 15132
Cincinnati 15, Ohio
Attn: J. A. McGurty

28. General Electric Company
Research Laboratory
One River Road
Schnectady, New York

29. General Electric Company
Special Purpose Nuclear System Operations
Vallecitos Atomic Laboratory
P. O. Box 846
Pleasanton, California
Attn: B. Voorhees

30. General Motors Corporation
Research Laboratories
GM Technical Center
12 Mile and Mound Roads
Warren, Michigan
Attn: F. E. Jamerson

31. General Telephone & Electronics Laboratories, Inc.
208-20 Willets Point Boulevard
Bayside 60, New York
Attn: R. Steinitz

32. Hughes Aircraft
3101 Malibu Canyon Road
Building 250
Malibu, California
Attn: R. C. Knechtli

33. Institute for Defense Analysis
Universal Building
1825 Connecticut Avenue, N. W.
Washington 9, D. C.
Attn: R. C. Hamilton

34. International Telephone & Telegraph Laboratories
3301 Wayne Trace
Fort Wayne, Indiana
Attn: Donald K. Coles

35. Jet Propulsion Laboratory
California Institute of Technology
4800 Oak Grove Drive
Pasadena, California
Attn: Arvin Smith
Peter Rouklove

36. Los Alamos Scientific Laboratory
P. O. Box 1663
Los Alamos, New Mexico (2 copies)
Attn: G. M. Grover

37. Marquardt Corporation
Astro Division
16555 Saticoy Street
Van Nuys, California
Attn: A. N. Thomas

38. Martin Marietta Corporation
Middle River
Baltimore, Maryland
Attn: M. Talaat

39. National Aeronautics & Space Administration
Western Operations Office
150 Pico Boulevard
Santa Monica, California
Attn: Fred Glaski

40. National Aeronautics & Space Administration
Manned Spacecraft Center
Houston, Texas
Attn: Librarian

41. National Aeronautics & Space Administration
1512 H Street, N. W.
Washington 25, D. C.
Attn: Fred Schulamn
James J. Lynch
George Deutsch
Walter Scott

42. National Aeronautics & Space Administration
Lewis Research Center
21000 Brookpark Road
Cleveland, Ohio 44135
Attn: Roland Breitwieser (C&EC)
Robert Migra (NRD)
Bernard Lubarsky (SPSD)
William J. LeGray (SPSD)
James J. Ward (SPSD)
J. W. R. Creagh (SPSD) (4 copies)
H. B. Probst (M&S)
J. F. Mondt (SPSD)
T. A. Moss (SPSD) (1 copy)
John J. Fackler (SPSPS)
R. Mather (SPSD)

43. National Aeronautics & Space Administration
Marshall Space Flight Center
Huntsville, Alabama
Attn: Librarian

44. National Aeronautics & Space Administration
Scientific & Technical Information Facility
Box 5700
Bethesda 14, Maryland
Attn: NASA Representative (2 copies + reproducible)

45. National Bureau of Standrads
Washington, D. C.
Attn: G. F. Rouse

46. Oak Ridge National Laboratory
Oak Ridge, Tennessee
Attn: Librarian

47. Office of Naval Research
Power Branch
Department of the Navy
Washington 25, D. C.
Attn: Cdr. J. J. Connelly, Jr.

48. Power Information Center
University of Pennsylvania
Moore School Building
200 South 33rd Street
Philadelphia 4, Pennsylvania

49. Pratt & Whitney Aircraft Corporation
East Hartford 8, Connecticut
Attn: William Lueckel
Ron Cohen

50. Radiation Effects Information Center
Batelle Memorial Institute
505 King Avenue
Columbus 1, Ohio
Attn: R. E. Bowman

51. Radio Corporation of America
Electron Tube Division
Martha and Marshall Avenues
Lancaster, Pennsylvania
Attn: Fred Block

52. Radio Corporation of America
David Sarnoff Research Center
Princeton, New Jersey
Attn: Karl G. Hernqvist

53. The Rand Corporation
1700 Main Street
Santa Monica, California
Attn: Librarian

54. Republic Aviation Corporation
Farmingdale, Long Island, New York
Attn: Alfred Schock

55. Space Technology Laboratories Inc.
One Space Park
Redondo Beach, California
Attn: Librarian

56. Texas Instruments Incorporated
13500 North Central Expressway
Dallas 22, Texas
Attn: R. A. Chapman

57. Thermo Electron Engineering Corporation
85 First Avenue
Waltham 54, Massachusetts
Attn: George Hatsopoulos

58. Thompson Ramo Wooldridge, Incorporated
7209 Platt Avenue
Cleveland 4, Ohio
Attn: W. J. Leovic

59. Union Carbide Corporation
Parma Research Center
12900 Snow Road
Parma, Ohio
Attn: Librarian

60. United Aircraft Corporation
Research Laboratories
East Hartford, Connecticut
Attn: R. Meyerand

61. United Nuclear Corporation
5 New Street
White Plains, New York
Attn: Al Strasser

62. U. S. Army Signal R & D Laboratory
Fort Monmouth, New Jersey
Attn: Emil Kittil

63. U. S. Atomic Energy Commission
Division of Reactor Development
Washington 25, D. C.
Attn: Auxiliary Power Branch
Direct Conversion Branch
Army Reactor Water Systems Branch
Isotopic Branch
SNAP Reactors Branch

63a. Mr. Socrates Christopher
Fuels and Materials Development Branch
AEC Headquarters
Germantown, Maryland

64. U. S. Atomic Energy Commission
Technical Reports Library
Washington 25, D. C.
Attn: J. M. O'Leary

65. U. S. Atomic Energy Commission
Department of Technical Information Extension
P. O. Box 62
Oak Ridge, Tennessee

66. U. S. Atomic Energy Commission
San Francisco Operations Office
2111 Bancroft Way
Berkeley 4, California
Attn: Reactor Division

67. U. S. Naval Research Laboratory
Washington 25, D. C.
Attn: George Haas
Librarian

68. University of Wisconsin
Madison, Wisconsin
Attn: Harold W. Lewis

69. Westinghouse Electric Corporation
Aerospace Department
Lima, Ohio
Attn: Harry Gray

70. Westinghouse Electric Corporation
Research Laboratories
Pittsburgh, Pennsylvania
Attn: R. J. Zollweg

71. Materials Research Corporation
Route 303
Orangeburg, New York 10962
Attn: Mr. V. E. Adler

72. Astro Met Associates, Incorporated
500 Glendale - Milford Road
Cincinnati, Ohio 45215

73. Monsanto Research Corporation
Station B, Box 37
Dayton, Ohio 45407
Attn: Wendell P. Bigony
Security Office